

## **Advanced Hot Gas Filter Development**

**Topical Report: Task 3 & Task 4  
September 29, 1994 to March 31, 1998**

**E. S. Connolly  
G. D. Forsythe**

**December 22, 1998**

**Work Performed Under Contract: DE-AC21-94MC31214  
DOE/FETC Project Manager: T. J. McMahon**

**For**

**U. S. Department of Energy  
Office of Fossil Energy  
Federal Energy Technology Center  
Morgantown, West Virginia**

**Prepared by**

**AlliedSignal Composites Inc. (formerly DuPont Lanxide Composites Inc.)  
1300 Marrows Road  
P. O. Box 9559  
Newark, DE 19714-9559**

## DISCLAIMER

This report was prepared as an account of work sponsored by the United States Government. Neither the United States nor the United States Department of Energy, nor any of their employees, makes any warranty, expressed or implied, or assumes any legal liability or responsibility for the accuracy, completeness, or usefulness of any information, apparatus, product, or process disclosed, or represents that its use would not infringe privately owned rights. Reference herein to any specific commercial product, process, or service by trade name, mark, manufacturer, or otherwise, does not necessarily constitute or imply its endorsement, recommendation, or favoring by the United States Government or any agency thereof. The views and opinions of authors expressed herein do not necessarily state or reflect those of the United States Government or any agency thereof.

## PATENT STATUS

In July 1997, a patent was filed which covered the development of an improved surface filtration membrane for hot gas filters. This patent was filed as a "continuation-in-part" to the original Hot Gas Filter Patent (5,460,637) owned by DuPont Lanxide Composites Inc. In September 1997, the United States Department of Energy granted DuPont Lanxide Composites Inc. a waiver request for the subject invention, DOE Docket No. S-88,782. In November 1998, this patent was approved by the United States Patent Office. At the time of this publication, the patent number had not yet been assigned.

## TECHNICAL STATUS

This technical report is being transmitted in advance of DOE review and no further dissemination or publication shall be made of the report without prior approval of the DOE Project/Program Manager.

## CONTRACTOR'S NOTE

Contract #DE-AC21-94MC31214 was awarded to DuPont Lanxide Composites Inc. in September 1994. In August 1998, DuPont Lanxide Composites Inc. was acquired by AlliedSignal Inc., and renamed AlliedSignal Composites Inc. Novation of this contract was performed by DCMC in January 1999.

## TABLE OF CONTENTS

<b>1. EXECUTIVE SUMMARY</b>	1
<b>2. INTRODUCTION</b>	2
<b>3. TECHNICAL RESULTS AND DISCUSSION</b>	5
<b>3.1 Background Technology</b>	5
<b>3.2 Material Qualification (Subtask 3.1)</b>	7
3.2.1 Improving the Surface Membrane	8
3.2.2 Development of a Dual Membrane Candle Filter	10
3.2.3 Mechanical Testing	12
3.2.4 Strengthened Flanges	15
3.2.5 Filtration and Permeability Testing	17
<b>3.3 Field Testing of "Baseline" PRD-66 Filter Elements</b>	19
3.3.1 Tidd Test Segment 4	19
3.3.2 Tidd Test Segment 5	20
3.3.3 Analysis of Field Exposed Elements (Subtask 3.4)	20
<b>3.4 Development of High Efficiency Membrane</b>	29
<b>3.5 Manufacturing Hot Gas Filters (Task 4)</b>	33
3.5.1 Raw Materials Plan (Subtask 4.1)	33
3.5.2 Process Instrumentation (Subtask 4.2)	33
3.5.3 Process Variables Experiments (Subtask 4.3)	34
3.5.4 Process Capability Demonstration (Subtask 4.4)	40
3.5.5 Equipment Analysis and Improvement (Subtask 4.5)	45
<b>3.6 Field Testing of "Improved" PRD-66 Filter Elements</b>	47
3.6.1 High Temperature High Pressure (HTHP) Testing at <u>W</u> -STC	47
3.6.2 PCFBC Exposure at Karhula	53
<b>4. CONCLUSIONS</b>	67
<b>5. RECOMMENDATIONS</b>	70
<b>6. ACKNOWLEDGMENTS</b>	71
<b>7. REFERENCES</b>	72

## LIST OF FIGURES

Figure 1 - Schematic of the basic process for winding PRD-66 cylindrical structures.-----	6
Figure 2 - Schematic of the PRD-66 membrane winding process.-----	6
Figure 3 - Phase diagram including PRD-66 composition.-----	7
Figure 4 - Impact of three PRD-66 variables on backpressure ( $\Delta P$ ), where "N" is the number of samples. ----	9
Figure 5 - Impact of inside diameter membrane on backpressure ( $\Delta P$ ), where "N" is the number of samples. -	11
Figure 6 - Typical Load Displacement Curve for PRD-66 filter segment.-----	12
Figure 7 - O-rings AFTER (left) and BEFORE (right) diametrical compression testing.-----	13
Figure 8 - Weibull Analysis of PRD-66 candle filter segment.-----	14
Figure 9 - Strain rate dependence of o-ring crushing test.-----	15
Figure 10 - O-ring diametrical compressive strength versus ring weight.-----	16
Figure 11 - O-ring diametrical compressive strength vs. amount & viscosity of infiltrate -----	16
Figure 12 - Load Displacement Curve for infiltrated PRD-66 filter segment.-----	17
Figure 13 - <u>W</u> -STC Room Temperature Gas Flow Resistance measurements of 1.5-meter PRD-66 filter elements with various membranes. <sup>12</sup> -----	18
Figure 14 - "Divots" in PRD-66 filter tested in Tidd Test Segment 5.-----	20
Figure 15 - White deposit (middle left) in vicinity of "divot" (upper right).-----	23
Figure 16 - Unit-cell size of magnesium sulfate versus state of hydration.-----	23
Figure 17 - Particle Infiltration Test (PIT) Device-----	25
Figure 18 - PIT-exposed sample viewed in transmitted light.-----	25
Figure 19 - Untested sample viewed in transmitted light.-----	25
Figure 20 - Exaggerated illustration of a PRD-66 delamination-----	26
Figure 21 - Original wound membrane (wall cross-section).-----	30
Figure 22 - Membrane with added filler (wall cross-section)-----	30
Figure 23 - Modified membrane with PIT rating of "10".-----	30
Figure 24 - Hole in membrane, undetectable under direct light.-----	31
Figure 25 - Hole in membrane, detectable under transmitted light.-----	31
Figure 26 - Hole in membrane after 25 PIT cycles, viewed in transmitted light.-----	31
Figure 27 - PRD-66M membrane, measured pore distribution.-----	32
Figure 28 - PRD-66M flow resistance for 1.5-meter candles.-----	32
Figure 29 - PRD-66C membrane, measured pore distribution.-----	32
Figure 30 - PRD-66C flow resistance for 1.5-meter candles.-----	32
Figure 31 - Impact of membrane weight and type on backpressure.-----	39
Figure 32 - PRD-66 Candle Filter dimensions-----	41
Figure 33 - Tip of original steel mandrel-----	46
Figure 34 - PRD-66C - Room temperature gas flow resistance <sup>12</sup> -----	48
Figure 35 - PRD-66M - Room temperature gas flow resistance <sup>12</sup> -----	48
Figure 36 - Gas flow resistance of as-manufactured and HTHP-exposed PRD-66M elements <sup>12</sup> -----	50
Figure 37 - Gas flow resistance of as-manufactured and HTHP-exposed PRD-66C elements <sup>12</sup> -----	50
Figure 38 - Karhula-exposed PRD-66C filters-----	54

Figure 39 - Outside diameter of Karhula-exposed element before ash removal	55
Figure 40 - Inside diameter of Karhula-exposed element before ash removal	55
Figure 41 - Differential pressure of Karhula filters measured by Foster Wheeler	56
Figure 42 - Wall interior of Karhula-exposed candle #577	57
Figure 43 - Close-up of #577 - OD surface and 1-2mm below	57
Figure 44 - 300X - UNEXPOSED candle surface	58
Figure 45 - 300X - EXPOSED candle surface	59
Figure 46 - 1,000X - EXPOSED candle surface	59
Figure 47 - UNEXPOSED CANDLE, cross-section of membrane filler (300X)	60
Figure 48 - EXPOSED CANDLE, cross-section of membrane filler (300X)	60
Figure 49 - 25X, fast-fracture - UNEXPOSED CANDLE, interior of support wall	61
Figure 50 - 25X, fresh-fracture - EXPOSED CANDLE, interior of support wall	61
Figure 51 - 50X, fast-fracture - UNEXPOSED CANDLE, interior of support wall	62
Figure 52 - 50X, fast-fracture - EXPOSED CANDLE, interior of wall support	62
Figure 53 - UNEXPOSED CANDLE, individual "yarn bundle" (300X)	64
Figure 54 - EXPOSED CANDLE, individual "yarn bundle" (300X)	64
Figure 55 - UNEXPOSED CANDLE, individual "yarn bundle" (1,000X)	65
Figure 56 - EXPOSED CANDLE, individual "yarn bundle" (1,000X)	65

## LIST OF TABLES

Table 1 - Impact of "intermediate" matrix ratio on backpressure ( $\Delta P$ ) at 5 scfm	10
Table 2 - Impact of dual membranes on backpressure ( $\Delta P$ ) at 5 scfm.	12
Table 3 - Average o-ring diametrical compressive strength ("n" is the number of samples).	14
Table 4 - Comparison of test conditions in Tidd Test Segments 4 and 5.	21
Table 5 - Process variables investigated for winding filter support.	35
Table 6 - Observed impact of process changes on support winding.	35
Table 7 - Impact of grit-size and binder content on backpressure.	38
Table 8 - Impact of binder content on backpressure of PRD-66C.	39
Table 9 - Process Capability Demonstration	42
Table 10 - Process Capability Summary	43
Table 11 - <u>W</u> -STC Room temperature and process strength of PRD-66 elements <sup>12</sup>	51
Table 12 - <u>W</u> -STC Ultimate load applied during strength characterization <sup>12</sup>	52
Table 13 - <u>W</u> -STC Material properties of PRD-66 elements <sup>12</sup>	52
Table 14 - DLC Diametrical compression testing of HTHP-exposed & unexposed candles	53
Table 15 - Karhula PCFBC test conditions	53
Table 16 - O-ring diametrical compressive testing of Karhula-exposed & unexposed candles	66

## 1. EXECUTIVE SUMMARY

DuPont Lanxide Composites, Inc. undertook a forty-month program, under DOE Contract DE-AC21-94MC31214, in order to develop hot gas candle filters from a patented material technology known as PRD-66. The goal of this program was to extend the development of this material as a filter element and fully assess the capability of this technology to meet the needs of Pressurized Fluidized Bed Combustion (PFBC) and Integrated Gasification Combined Cycle (IGCC) power generation systems at commercial scale.

The principal objective of Task 3 was to build on the initial PRD-66 filter development, optimize its structure, and evaluate basic material properties relevant to the hot gas filter application. Initially, this consisted of an evaluation of an advanced filament-wound core structure that had been designed to produce an effective bulk filter underneath the barrier filter formed by the outer membrane. The basic material properties to be evaluated (as established by the DOE/METC materials working group) would include mechanical, thermal, and fracture toughness parameters for both new and used material, for the purpose of building a material database consistent with what is being done for the alternative candle filter systems. Task 3 was later expanded to include analysis of PRD-66 candle filters, which had been exposed to actual PFBC conditions, development of an improved membrane, and installation of equipment necessary for the processing of a modified composition.

Task 4 would address essential technical issues involving the scale-up of PRD-66 candle filter manufacturing from prototype production to commercial scale manufacturing. The focus would be on capacity (as it affects the ability to deliver commercial order quantities), process specification (as it affects yields, quality, and costs), and manufacturing systems (e.g. QA/QC, materials handling, parts flow, and cost data acquisition).

## 2. INTRODUCTION

Advanced, coal-based power plants will require durable and reliable hot gas filtration systems to remove particulate contaminants from the gas streams to protect downstream components such as turbine blades from erosion damage. It is expected that the filter elements in these systems will have to be made of ceramic materials to withstand goal service temperatures of 1600°F or higher. Recent demonstration projects and pilot plant tests have indicated that the current generation of ceramic hot gas filters (cross-flow and candle configurations) are failing prematurely. Two of the most promising materials that have been extensively evaluated are clay-bonded silicon carbide<sup>1,2</sup> and alumina-mullite porous monoliths. These candidates, however, have been found to suffer progressive thermal shock/fatigue damage, as a result of rapid cooling/heating cycles. Such temperature changes occur when the hot filters are back-pulsed with cooler gas to clean them, or in process upset conditions, where even larger gas temperature changes may occur quickly and unpredictably.<sup>9</sup> In addition, the clay-bonded silicon carbide materials are susceptible to chemical attack of the glassy binder phase that holds the SiC particles together, resulting in softening, strength loss, creep, and eventual failure.<sup>1</sup>

To address these issues, Du Pont Lanxide Composites (DLC) developed a unique and innovative new candle filter made from a ceramic material called PRD-66. This material, an extensively microcracked structure comprising a mixture of crystalline oxide phases (primarily mullite, cordierite, and corundum). It combines the high chemical stability inherent in the oxide ceramics with a thermal shock resistance typically found only in state-of-the art, fiber-reinforced, ceramic matrix composites. The highly microcracked structure provides an effective mechanism for stopping crack propagation through the material, resulting in a toughened structure that responds to high impacts, that would cause catastrophic brittle fracture in monolithic structures, by forming dents.<sup>7</sup>

An additional attribute of PRD-66 ceramic structures is that unlike many whisker-reinforced ceramic composites, they contain no respirable ceramic fibers. This makes handling, installation, and removal of the filters a simpler task, requiring no special protective equipment or record keeping, necessary to comply with the increasing health concerns and likely regulations governing personnel exposure to non-asbestos respirable fibers (NARFS).<sup>7</sup>

Based on its low-cost ingredients and relatively simple manufacturing process, commercial quantity costs of PRD-66 hot gas filters are expected to be fully competitive with the clay-bonded SiC and alumina-mullite monolithic filters that have been involved in recent demonstration programs.

Prototype PRD-66 candle filters are comprised of a cleanable porous membrane structure over a core that is inherently a bulk filter. Should the membrane become locally damaged by an impact e.g., during installation. The exposed core structure would continue to filter out particulates, until it eventually "blinds", effectively healing the damaged section while the rest of the filter continues to perform as designed.

Early development activity included a preliminary material characterization and the demonstration of acceptable permeability and dust retention properties. One-meter working prototypes were manufactured and tested in cooperation with Westinghouse Science and Technology Center.<sup>2</sup> Testing included short-term, high temperature, high pressure exposure to simulated Pressurized Fluidized Bed Combustion conditions under steady state and thermal transients (accelerated pulse cleaning and turbine trip simulations). Although limited, this testing was sufficiently encouraging to stimulate production of 1.5-meter prototypes with a flange configuration that was designed to allow retrofit in existing demonstration units.

Based on the initial development successes of PRD-66 hot gas candle filter prototypes,<sup>2</sup> the goal of this program was to extend the development of PRD-66 candle filters and fully assess the capability of this technology to meet the needs of PFBC and IGCC power generation systems at commercial scale. The work will emphasize optimizing the filter body and flange configurations, demonstrating goal mechanical durability in qualification testing under normal and "upset" operating conditions, and defining and addressing the key issues involved in manufacturing PRD-66 hot gas filters at commercial scale.

The scientific and engineering rationale for developing PRD-66 as a hot gas filtration media is supported by the following evidence:

- ◆ The chemical stability of these oxides in coal combustion environments is well known.<sup>3</sup>
- ◆ PRD-66 has an extended use temperature of over 1200 degrees Celsius (2200° F). This service temperature significantly exceeds the goals of current coal combustion programs, and keeps the way open to higher temperature higher thermodynamic efficiency combustion processes in the future.<sup>7,8</sup>
- ◆ Microcracked structures such as this, in addition to being inherently porous filtering structures, are very effective at preventing crack propagation. Because of this microstructure, the thermal shock resistance of PRD-66 is outstanding. In catalyst support applications PRD-66 was subjected to multiple thermal downshocks (theoretically exceeding 10,000°C/second) in turbine trip simulations without damage.<sup>7,8</sup>

- ◆ By using highly developed textile and composite forming technologies, the precise location of each yarn can be controlled and structures fabricated with independent control of gas paths, porosities, and backpressure. This allows for the creation of filters having a thin, low pressure drop surface barrier, backed up by a bulk-filter core that acts as a secondary, backup filter to protect the turbine, should the filter surface be mechanically damaged during installation or operation.<sup>7,8</sup>
- ◆ The manufacturing process is environmentally clean and neither uses nor generates hazardous chemicals or respirable fibers.
- ◆ The manufacturing process is simple, well controlled, and readily scaleable.
- ◆ The ingredients (fiberglass yarn and alumina) are inexpensive and readily available. This offers a route to advanced filters that will be price competitive with the current generation of hot gas filters.<sup>7,8</sup>
- ◆ DLC has installed capacity that is sufficient to meet the industry's development needs for the next several years. Capacity can be readily expanded with minimal new investment. This offers a clear path to scale-up without requiring the industry to support large capital investments or wait a long time to evaluate or adopt the technology on a commercial scale.

### 3. TECHNICAL RESULTS AND DISCUSSION

#### 3.1 Background Technology

PRD-66 all-oxide ceramic materials were invented and patented by DuPont and assigned to Du Pont Lanxide Composites (DLC), a joint venture company owned by E. I du Pont de Nemours, Inc. and Lanxide, Inc. A fiberglass yarn is coated with a suspension of alumina in water, and placed by high precision fiber handling techniques, in this case, filament winding, into the net shape of the filter. This preform is allowed to dry, then fired through a proprietary firing cycle. In this firing process, the silica and magnesia in the fiberglass react with the alumina in the slurry to form mullite and cordierite. The surface of the material is unreacted alumina. It should be noted that the fiberglass is consumed in this chemical reaction, and the resulting product is not fiber reinforced.<sup>7</sup>

For several years prior to the initiation of this project, DuPont, DLC, and Westinghouse Electric Corporation cooperated in the fabrication and early testing of hot gas candle filters based on the PRD-66 technology. The result of that collaboration will, hereafter in this report, be referred to as the "baseline" PRD-66 Candle Filter.

The raw materials required to produce a "baseline" PRD-66 Candle Filter are fiberglass yarn (S-2 type, produced by Owens Corning), calcined alumina power (A-17, produced by Alcoa), fumed alumina powder (produced by Degussa), and deionized water.

The flange, body and membrane portions of the PRD-66 Candle Filter are all produced by coating the fiberglass yarn with a precise amount of alumina slurry and winding the coated filament onto a spinning mandrel.<sup>7</sup>

The first step in producing a PRD-66 Candle Filter is the fabrication of the flange segment. This operation is performed, as shown in Figure 1, on a small winder (max. unit length = 6 inches). The slurry-coated yarn is wound onto a 46mm diameter mandrel with a removable plastic sleeve. When the cylindrical structure is 60mm in diameter, the winding is stopped. The "integral flange" and the plastic sleeve are then removed from the flange mandrel, and slid onto the filter mandrel, which had been previously covered with a plastic sleeve along its entire length. The integral flange is positioned at the appropriate position from the tip end of the mandrel.

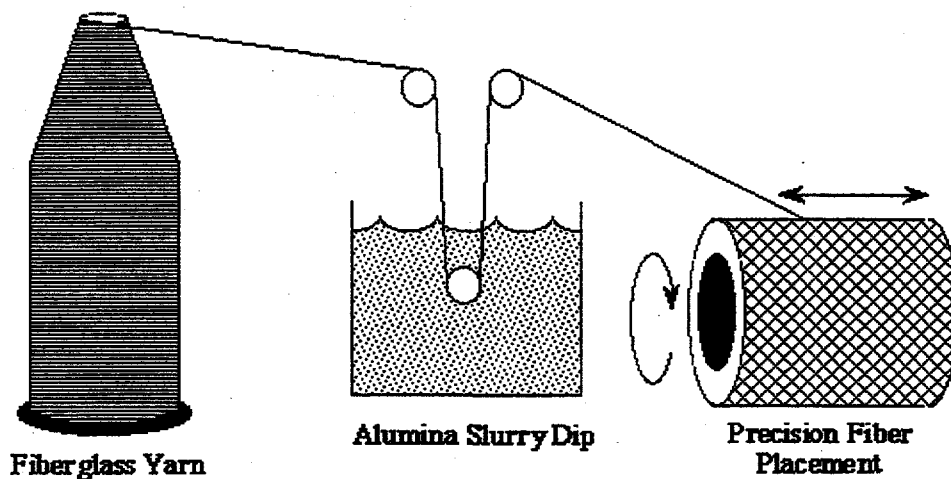


Figure 1 - Schematic of the basic process for winding PRD-66 cylindrical structures.

The winding of the filter support is then performed, as shown in Figure 1, on a winder capable of producing 65-inch long cylindrical structures. As the slurry-coated yarn is applied to the mandrel, it encases the integral flange. Winding proceeds until the outside diameter of the tube is 60mm, yielding a flange diameter of 74mm.

The winding of the membrane yarn is then performed, as shown Figure 2, on a winder which has been specially designed for laying down the yarn at approximately 90° to the axis of the mandrel. The winding begins at the tip end of the candle support structure; each successive "hoop" is laid down immediately adjacent to the previous one. Winding proceeds along the straight portion of the filter, then over the flange portion of the filter, creating a single layer of membrane yarn.

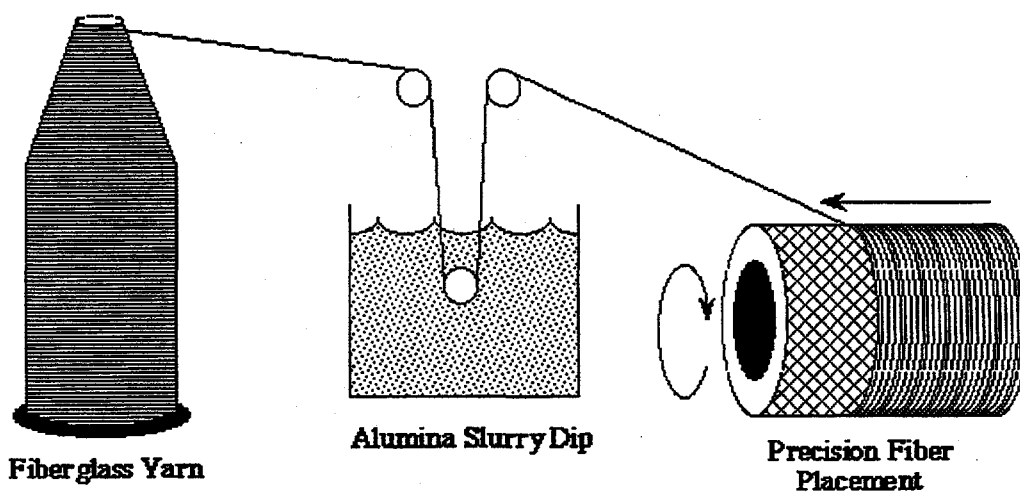


Figure 2 - Schematic of the PRD-66 membrane winding process.

The filter is then dried overnight on the mandrel, cut to length, and removed from the mandrel. A paste-like substance (comprised of the same raw materials as the filter itself) is then used to fill the hole left in the tip of the candle by the mandrel. The filter is then heated to approximately 1400°C in air. During this firing, the alumina coating reacts with the silica, magnesia, and alumina in the glass yarn to form a layered, microcracked structure comprising primarily cordierite, mullite, and corundum.

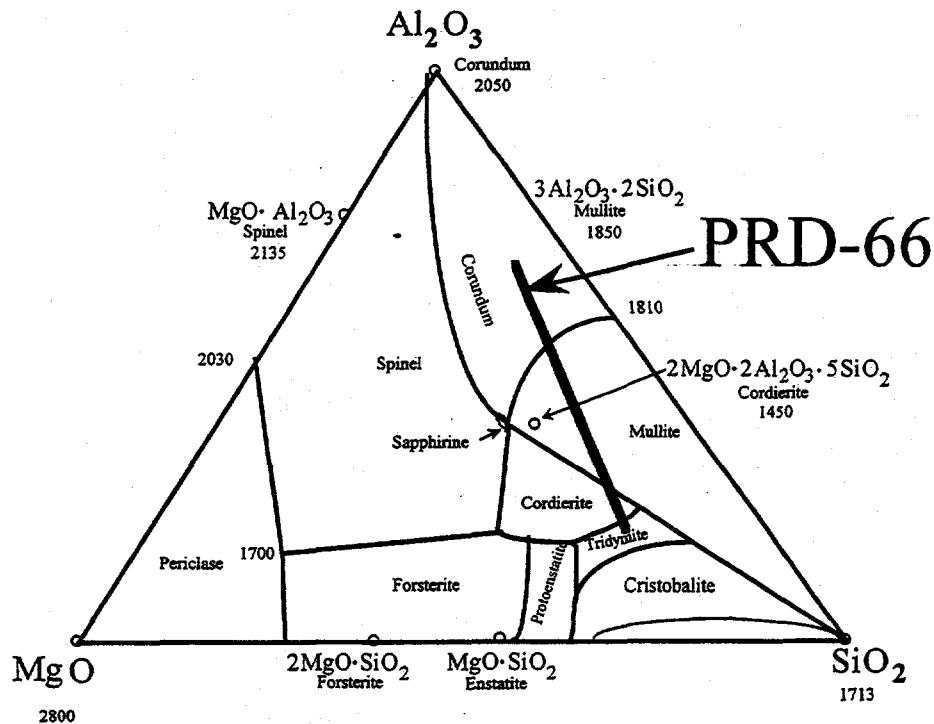


Figure 3 - Phase diagram including PRD-66 composition.

This "baseline" PRD-66 filter was successfully tested in Ohio Power's TIDD PFBC facility in the late summer through early fall of 1994.<sup>2</sup>

### 3.2 Material Qualification (Subtask 3.1)

In Subtask 3.1, attempts were made to improve the design of the baseline candle filter. The design improvements sought included:

1. improved surface filtration membrane for reduced pressure drop
2. a "dual membrane" filter (with membranes on the inside and outside surfaces) having acceptable backpressure
3. increased strength of the flange region

Full size candle filters, which incorporated these attempts at design changes, were fabricated. These filters were then tested by our subcontractor, Westinghouse Science and Technology Center, to assure that the improved filters still met the fundamental requirements of acceptable permeability and filtration efficiency. After this testing, a decision on which improvements were successful were made, and full sized candle filters incorporating the selected improvements were produced for testing in subsequent tasks.

Also in Subtask 3.1, mechanical property tests suitable for monitoring progress toward stronger filters, and ultimately for process control, were surveyed. After choosing the best test, the mechanical properties of the baseline filter were determined and an evaluation of strength improvements was performed.

### *3.2.1 Improving the Surface Membrane*

In attempting to improve the surface filtration membrane on the PRD-66 candle filter, while retaining good filtration characteristics, two properties had to be considered. Firstly, a lower backpressure membrane is desirable. Secondly, a membrane that will release the ashcake more easily is desirable. In the grossest qualitative sense, a smooth appearance on the surface of the filter is thought to be important to good cake release, and can be assessed visually. In the absence of an effective quantitative test, DLC attempted to maintain the same degree of smoothness in the membrane based on visual appearance. DLC had equipment in house to determine if a reduction in backpressure has been achieved and efforts concentrated on reducing the backpressure of the surface membrane.

There were essentially three "knobs" to turn in an attempt to reduce the backpressure of the membrane. They were the type of yarn used in the construction, the ratio of alumina slurry-to-yarn (the matrix ratio), and the spacing of the yarns on the surface of the filter body. Experiments were carried out to turn all three of these knobs in a systematic manner. The results of those experiments are presented in Figure 4.

To vary the yarn type, we chose to hold yarn denier constant at the level in the baseline filter, and vary the yarn twist. The two variations chosen are a twisted yarn and an untwisted yarn. It was expected that the untwisted yarn would flatten on the filter surface yielding a smoother membrane. The matrix ratio is determined by the size of the orifice in a stripper die, which controls the amount of alumina slurry applied to the yarn. To retain proprietary information regarding our process, we'll describe the matrix ratio values as "low" and "high." Finally, we can control the spacing of the surface yarns by adjusting the speed at which the yarn is wrapped around the support. To control

proprietary information, we will refer to these yarn spacing as "A" and "B," where "B" has fewer wraps per inch and a larger space between yarns. In these terms, the baseline filter membrane would be described as having been made with twisted yarn, high matrix ratio, and yarn spacing "A".

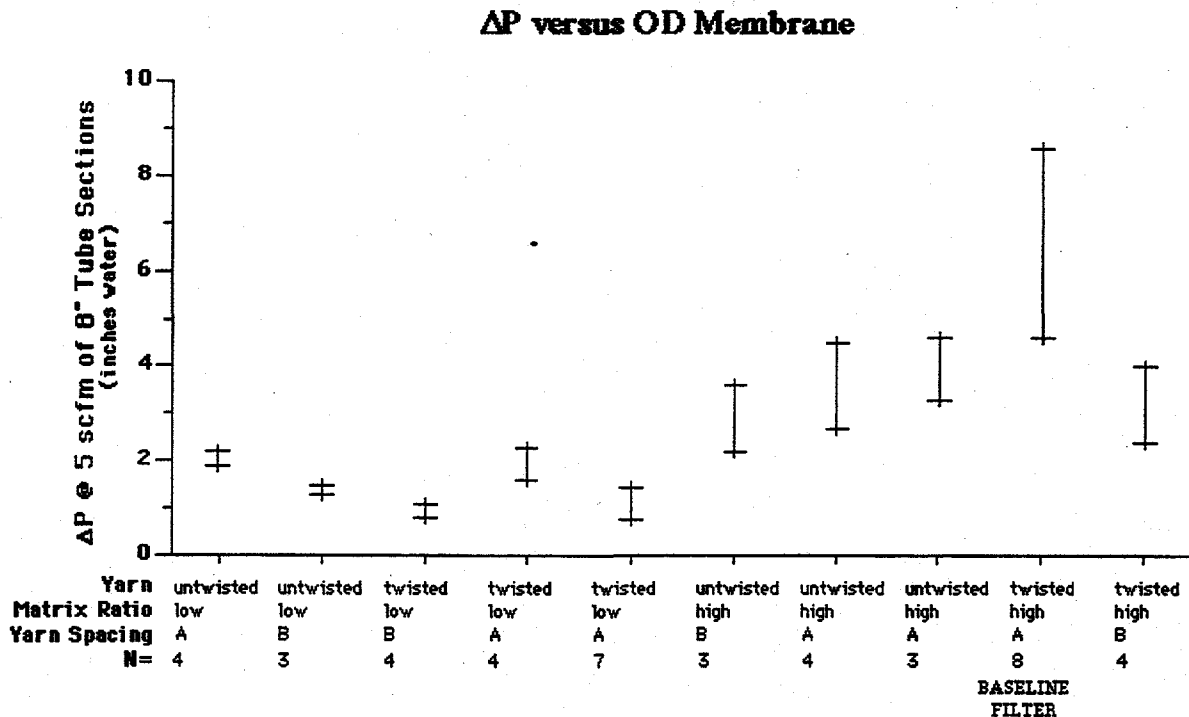


Figure 4 - Impact of three PRD-66 variables on backpressure ( $\Delta P$ ), where "N" is the number of samples.

As seen in Figure 4, every combination of yarn twist, matrix ratio, and yarn spacing examined in these experiments resulted in a reduction in backpressure when compared to the baseline filter. In these experiments, the new combinations were also less variable than the baseline filter. It should be noted that the backpressure measurements were made on 8" long samples taken from full size filters; the backpressure values presented in Figure 4 ARE NOT EQUAL TO values found on full filters, but they are proportional to them, so comparisons are meaningful.

There is no apparent correlation with yarn type seen in the data, a mild correlation with yarn spacing, and a strong correlation with matrix ratio. Lower matrix ratios have less alumina on the yarns, which probably results in less matrix bridging between adjacent yarns, and a more permeable membrane. It could not be determined if this "lower matrix ratio membrane" would provide an acceptable surface filtration. If it did, the results of these experiments indicate a reduction of surface membrane backpressure by a factor of four is possible.

The choice of yarn spacing is less clear. Yarn spacing 'B' generally gave slightly lower backpressure, but resulted in a visual appearance with randomly spaced gaps in the membrane. These gaps are likely to provide dust leak paths, and therefore poor filtration performance and may adversely effect cake release. DLC, therefore, elected to forego the small drop in backpressure and remain with the baseline yarn spacing.

The untwisted yarn did flatten on the surface of the filter body as anticipated, but was more difficult to manufacture, leading to lower yields and higher costs. It also did not lead to an additional improvement in backpressure when used with the low matrix ratio.

Based on these results, DLC recommended the combination of a twisted yarn, low matrix ratio, and yarn spacing A, because of the low backpressure, retention of a smooth membrane, and ease of manufacture of such filters. DLC manufactured two filters having these parameters for examination by Westinghouse Science and Technology Center; results are discussed in "3.2.5 Filtration and Permeability Testing".

Serious concerns were raised by Westinghouse over poor adhesion of the reduced backpressure membranes. In response, test were conducted with an intermediate matrix ratio, which was more adherent, but still had significantly lower backpressure then the baseline filter; data is shown below in Table 1. New samples were produced for testing; two-inch segments were cut from three locations (flange end, middle, and closed end). Each was sealed around the cut edge and shipped to W-STC for bench-scale permeability and particle filtration efficiency testing.

Position within Candle	$\Delta P$ of 8" Segment (iwg, inches-water gauge)	$\Delta P$ of 8" Baseline Segment (iwg, inches-water gauge)
Flange End	2.4	4.7
Mid-Candle	2.0	5.8
Tip End	2.2	5.3

Table 1 - Impact of "intermediate" matrix ratio on backpressure ( $\Delta P$ ) at 5 scfm

### 3.2.2 Development of a Dual Membrane Candle Filter

During earlier development efforts, Westinghouse expressed a desire to have a membrane along the inside, as well as outside, surfaces of the filter element; this configuration was referred to as a "dual membrane" filter. As a starting point for experiments leading to a "low backpressure, dual membrane" hot gas candle filter, we wound a bulk filter body identical to the baseline filter body, but with no inner or outer membrane. As shown below in Figure 5, this filter segment has an extremely low backpressure. This demonstrates that overall filter backpressure is dominated by the pressure

drop at the surface membranes. Efforts were focused, therefore, on developing a “low backpressure, dual membrane” filter with “low pressure drop” outside diameter membranes.

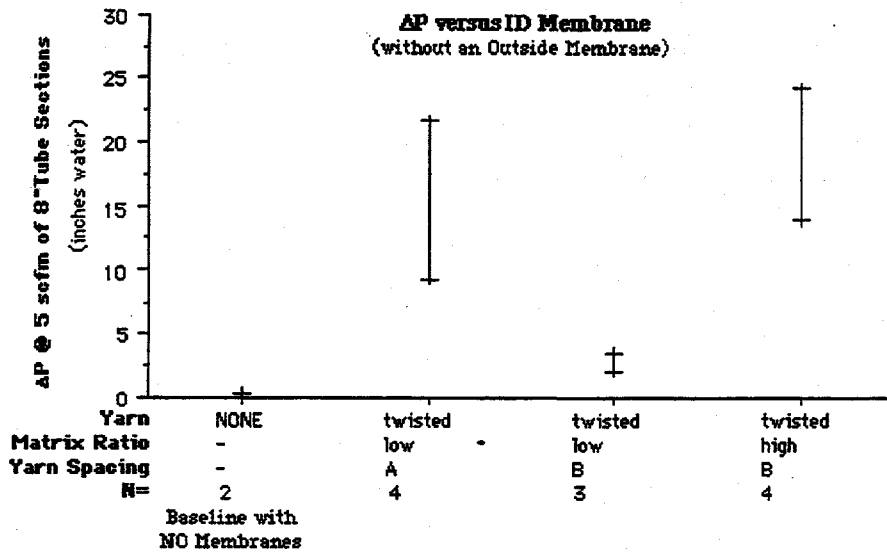


Figure 5 - Impact of inside diameter membrane on backpressure ( $\Delta P$ ), where “N” is the number of samples.

In a manner similar to the experiments described above, experiments were completed to fashion an internal membrane by the same filament winding techniques used for the outer membrane. Instead of winding on the outer body of the candle filter, the internal membrane is wound on the mandrel, and the body of the candle is wound on top of the membrane. Since the wet yarns conform to the surface of the smooth mandrel, a very smooth membrane surface is obtained. We therefore expect excellent cake release from this inner membrane.

Figure 5 shows a backpressure dependence of inner membranes on both “matrix ratio” and “yarn spacing”. No winding conditions could be found which would allow us to make a satisfactory inner membrane with an untwisted yarn. No gaps were formed in the membrane with yarn spacing “A” or “B”. The combination of twisted yarns, low matrix ratio, and yarn spacing “B” for the inner membrane, was chosen based on the low backpressure.

Samples of a dual membrane filter using these conditions for the inner membrane and the “medium matrix membrane” conditions described earlier are shown in Table 2.

Position within Candle	$\Delta P$ of 8" Segment (iwg, inches-water gauge)	$\Delta P$ of 8" Baseline Segment (iwg, inches-water gauge)
Flange End	6.3	4.7
Mid-Candle	9.9	5.8
Tip End	10.3	5.3

Table 2 - Impact of dual membranes on backpressure ( $\Delta P$ ) at 5 scfm.

### 3.2.3 Mechanical Testing

In order to judge the effectiveness of our experiments to strengthen the flange region of our filters, a reliable mechanical property test was necessary. It was desirable for such a test to minimize the effect of machining damage incurred in fashioning the test specimen, and to be amenable for quality control in future production. Because PRD-66 hot gas filters are made by a process that produces only tubular shapes, it was impossible to manufacture a flat coupon that closely mimicked the internal structure of a PRD-66 filter. Only tests that use cylindrical samples, therefore, were considered. This limited the range to o-ring or c-ring tests. C-ring tests were subjectively evaluated, but cutting the 1-inch slot from the coupon incurred machining damage and an additional fixturing cost would have been necessary to achieve reproducible slot geometries. O-ring tests were ideal in that they required only two, easily controllable cuts to sample a tubular product. Since o-ring tension tests require more complicated and costly fixtures, a simple o-ring compression test was most favored. Figure 6 shows a load deflection curve typical of the o-ring compression tests carried out in this project.

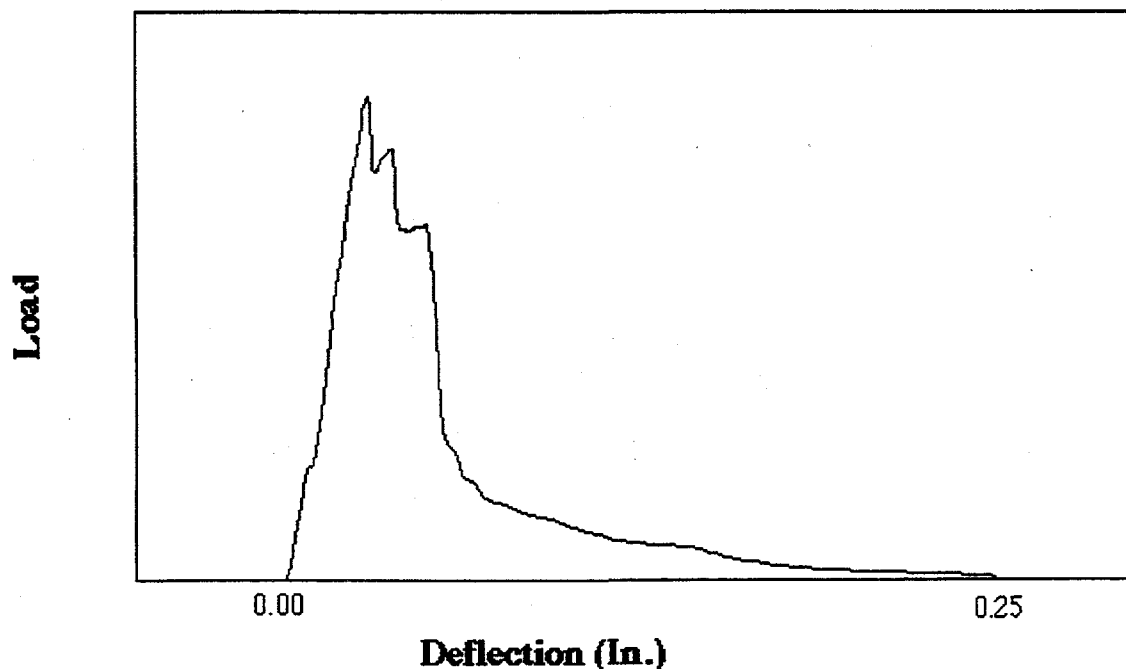


Figure 6 - Typical Load Displacement Curve for PRD-66 filter segment.

This displacement curve reveals a great deal of reloading and strain tolerance after peak load is achieved. Tests that were carried out until essentially no load resistance was encountered often had deflections as high as 0.25 inches, or roughly the same as the wall thickness of the sample. As shown in Figure 7, the samples were intact, though macroscopic cracks were readily visible. In the 100 or so mechanical tests conducted in developing this o-ring diametrical compression test, no sample fractured instantly into two or more pieces.

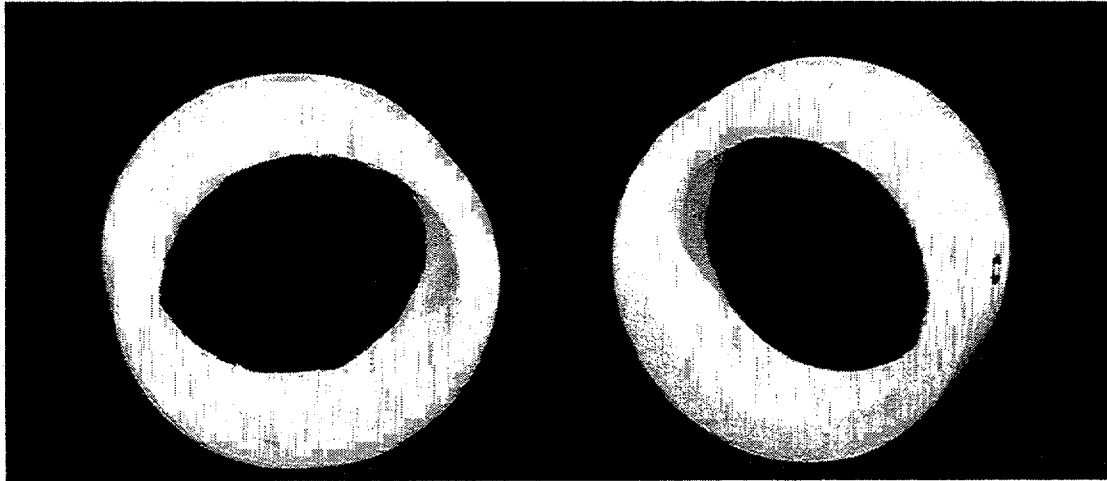


Figure 7 - O-rings AFTER (left) and BEFORE (right) diametrical compression testing.

The diametrical compressive strength was determined by the maximum peak at which the first crack occurred. To characterize PRD-66, forty-one 1-inch wide samples, from three different production filters were tested. The average crushing strength on the samples was 410 psi (std.dev. = 38 psi). This is significantly lower than the results of Westinghouse Science and Technology Center's tests, which reported strengths of 1050 psi on 3/4" wide o-rings. Unfortunately, the DLC records, which detailed the exact calculations used, were not available, however, a more accurate equation was adopted approximately a year after the original data was generated. In the later equation, developed by O.M. Jadaan, et al.<sup>10</sup>, stress is defined as follows:

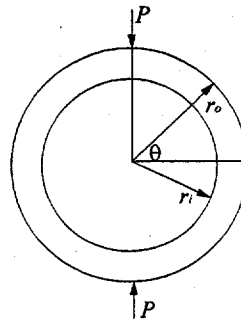
$$\sigma_{\theta} = \frac{P}{2} \left[ 0.637 \frac{r_o y}{I} - \cos(\theta) \left( \frac{1}{A} + \frac{r_o y}{I} \right) \right]$$

$$\text{where } I = \frac{1}{12} b(r_o - r_i)^3 = \frac{1}{12} bt^3$$

$$y = r_o - r$$

$$A = b(r_o - r_i) = bt$$

$$P = \text{load}$$



Where  $I$  is the moment of inertia,  $t$  is the thickness, and  $A$  is the cross-sectional area.

Using the new equation, a sample of the old data was recalculated as shown in Table 3. These strength values agree much better with data reported at W-STC. All data analysis that was conducted during Task 3, however, was performed with the old equations, which yielded lower values.

	Load (lbs)	Old Strength Value (psi)	New Strength Value (psi)
Filter #316 (n=13)	33	417	1057
Filter #317 (n=16)	35	369	934
Filter #318 (n=16)	41	423	1071

**Table 3 - Average o-ring diametrical compressive strength ("n" is the number of samples).**

A Weibull analysis, shown in Figure 8, was conducted on the original data after calculating the failure strengths of each of the o-rings at the point of maximum stress on the load/deflection curve (Figure 6). The resulting failure stresses were then used to obtain parameter estimates associated with the underlying population distribution.<sup>11</sup> PRD-66 behaved as expected for a porous ceramic material, with a Weibull modulus around "4". Significantly more data would be necessary to correct for statistical bias errors and calculate confidence bounds.

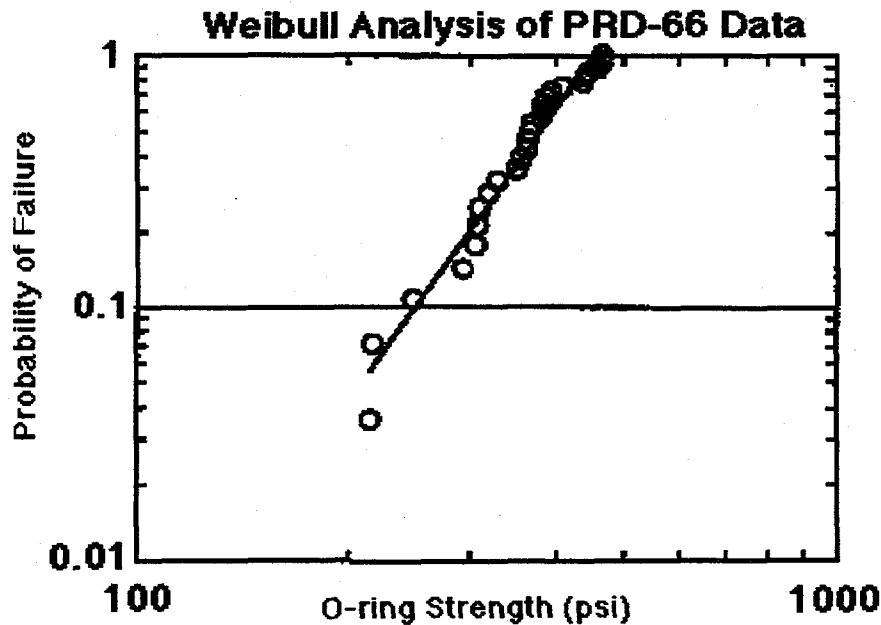


**Figure 8 - Weibull Analysis of PRD-66 candle filter segment.**

Additional o-rings were tested at various rates of applied stress, as determined by the crosshead speed of the apparatus. When the average strengths were plotted in Figure 9, there was no obvious strain rate dependence for PRD-66, additional data would be required, however, to verify statistical significance.

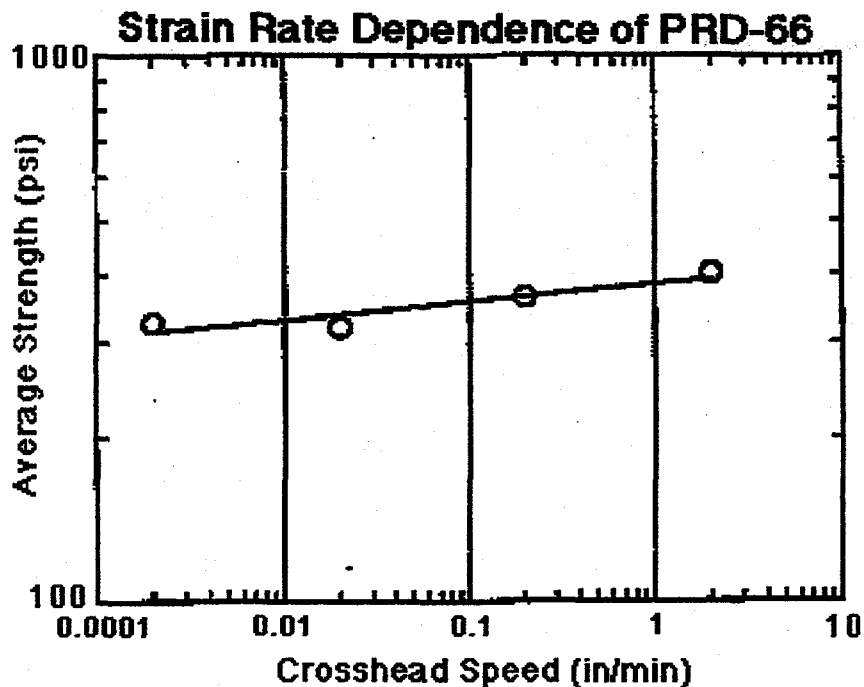


Figure 9 - Strain rate dependence of o-ring crushing test.

### 3.2.4 Strengthened Flanges

In previous experiments, it had been shown (although somewhat qualitatively) that selective reinforcement of PRD-66 filters can be obtained by adding slurry to portions of the filter in need of reinforcement after winding the filter body. This was of particular importance in view of early tests conducted at Westinghouse (and reported verbally to DLC) in which failure of the filter element occurred just below the flange. Since that time, the holder assembly was redesigned by W-STC and a method was developed by DLC to add controlled amounts of slurry to the areas requiring reinforcement.

Filter samples were fabricated with a range of slurry additions (10, 15, or 20 cc) introduced to portions of the bulk filter body. Three different slurry viscosities were also tested to examine whether the infiltrated slurry stayed where it had been applied or migrated into adjacent regions. To control for filter-to-filter variations, replicate samples were taken from several different filter bodies, and at different points along the body.

As seen in Figure 10 and Figure 11, there is a strong positive correlation between both the "weight gain" and "volume of added slurry" with o-ring crushing strength of 1-inch segments of the filter. Overall, strength increased from about 400 psi for uninfiltrated sections to about 600 psi for fully infiltrated samples, about a 50% increase in strength.

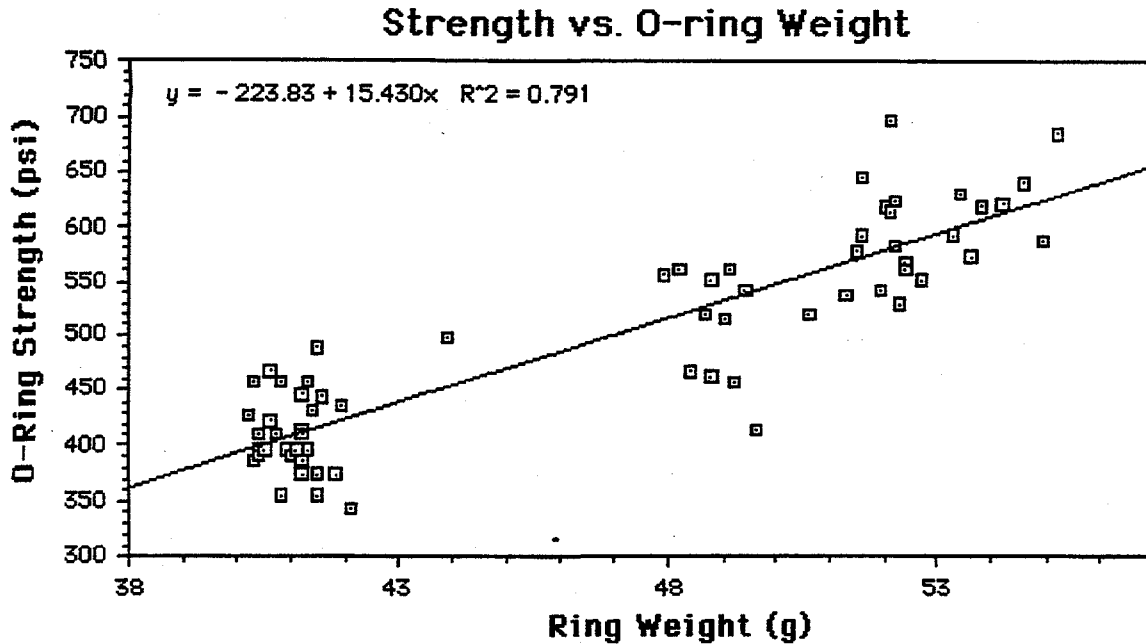


Figure 10 - O-ring diametrical compressive strength versus ring weight.

Higher viscosity slurries (Figure 11) achieved higher strengths with less slurry addition, and lower viscosities took more slurry to attain the same strength. This is probably due to migration of the slurry out of the test segment into the regions adjacent to it, which would result in less effective reinforcement.

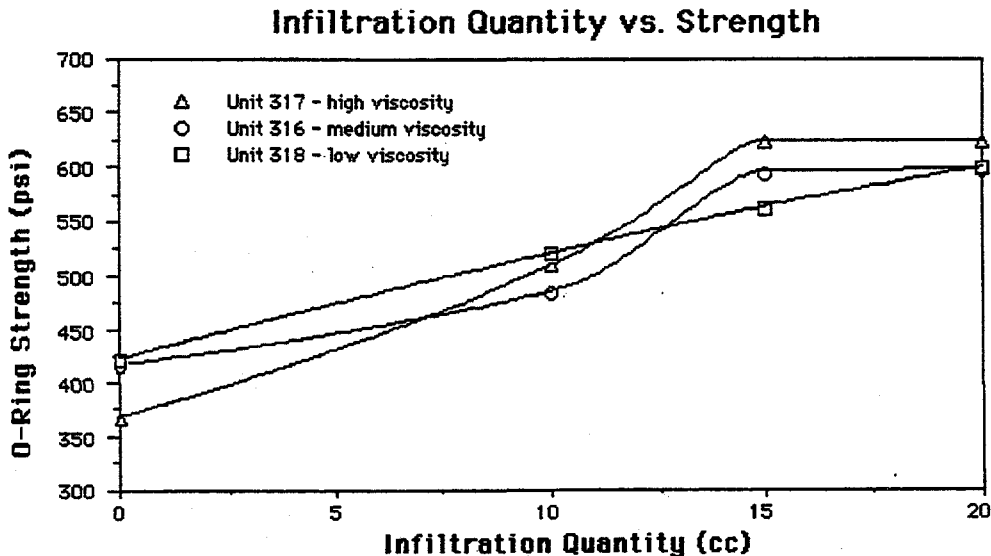


Figure 11 - O-ring diametrical compressive strength vs. amount & viscosity of infiltrate

There appears to be a greater tendency toward brittle failure with the infiltrated material, but, as shown in the load displacement curve of Figure 12, there is still quite graceful failure. We interpret the more triangular shape plot after maximum load (compared to Figure 6) as an indication

of more brittle failure, but the fact that there is significant reloading after "peak load" still suggests graceful failure. As with the uninfiltreated material, these samples never broke into two pieces, even with deflections as large as 1/4 inch and as many as four independent cracks per specimen.

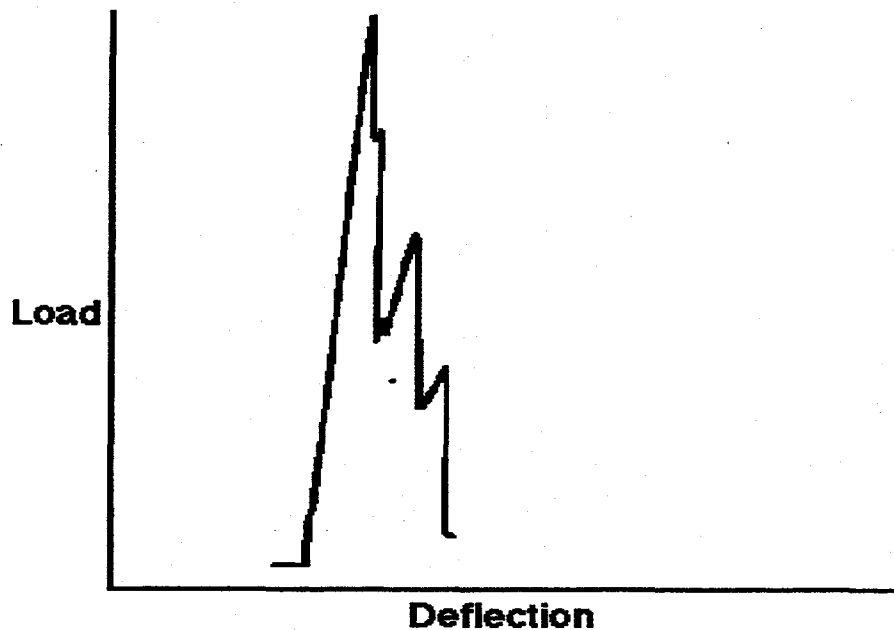


Figure 12 - Load Displacement Curve for infiltrated PRD-66 filter segment.

Seeing no real negative factors in using this new infiltration technique, and a significant benefit, strengthened flanges were incorporated into all three of the improved filter designs, mentioned earlier. Two "baseline" candles with the improved reinforcement technique at the flange were submitted to Westinghouse for testing.

### 3.2.5 Filtration and Permeability Testing

(Note: the following information, with regard to testing performed by Westinghouse Science and Technology Center (W-STC), was conducted under a subcontract between DLC and Westinghouse, a full copy of the Final Report is provided in Appendix 2.)

Preliminary tests were conducted by Westinghouse Science and Technology Center on 2-inch long filter segments that had low pressure and dual membranes. Dust was delivered to each sample's outside diameter at room temperature for ~3 minutes. Both the clean ID appearance, as well as the absence of detectable fines in the off-gas stream indicated excellent particle collection efficiency, by Westinghouse standards. When a tested specimen was fast-fractured, fines were evident below the outside diameter surface. Penetration within the 7-mm thick wall was apparent to a depth of 1 to 3 mm.

As mentioned earlier, DLC fabricated the following 1.5-meter candles for testing: two with improved (low pressure) outside membrane only, two dual membrane candles, and two "baseline" candles, ALL with strengthened flanges. Westinghouse performed room temperature gas flow resistance measurements on all six candles; results are show in Figure 13. These results parallel measurements conducted at DLC.

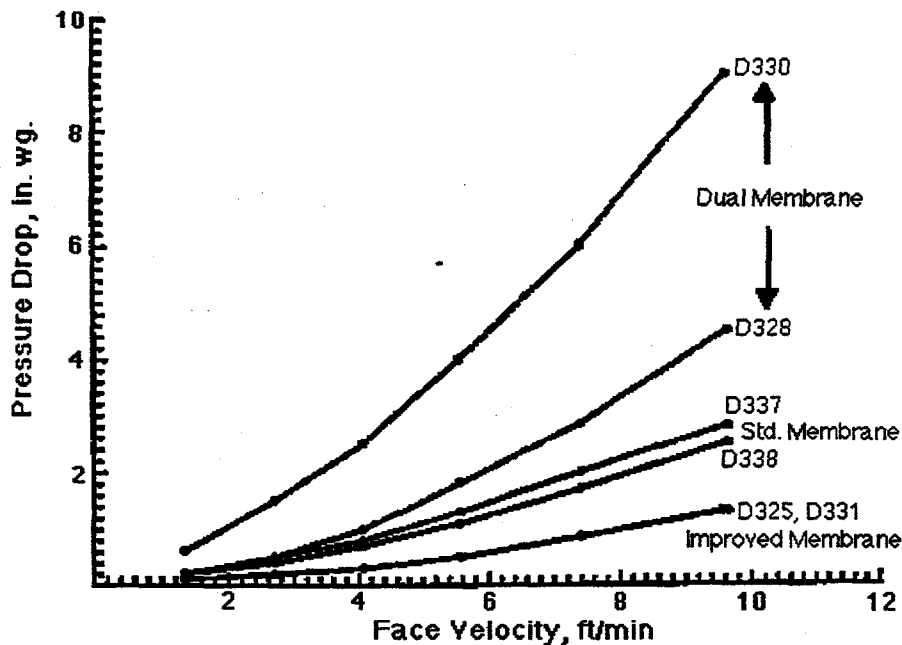


Figure 13 - W-STC Room Temperature Gas Flow Resistance measurements of 1.5-meter PRD-66 filter elements with various membranes.<sup>12</sup>

Westinghouse concluded that the "baseline" and the reduced backpressure membrane filters had flow restrictions within their specification range. The flow restriction of the two dual membrane filters did not agree with each other and one exceeded the pressure drop specification of <1 in-wg/fpm.

After two hours of high temperature exposure in Westinghouse's HTHP facility, outer membranes on the reduced backpressure and dual membrane filters delaminated. This was the most probable failure mode of these candles. The "strengthened flange" filter, which had the baseline surface membrane, did not delaminate.

### **3.3 Field Testing of "Baseline" PRD-66 Filter Elements**

Prior to the beginning of this program, PRD-66 hot gas candle filters (baseline filters) were tested at Westinghouse Electric Corporation's Science and Technology Center.<sup>2</sup> Testing on two-inch filter segments confirmed that PRD-66 filters had acceptable particle filtration efficiency and permeability characteristics in lab scale testing. Westinghouse then exposed full-size, 1.5-meter candle filters to simulated coal combustion filtration conditions in their high temperature high pressure (HTHP) test chamber. That testing confirmed that full-scale candle filters also performed well in filtration efficiency and permeability. Accelerated pulsing and process interruption testing revealed the need for strengthening of the flange region of the filter. After DLC took steps to increase the strength of the filter's flange, further accelerated tests which simulated 6000 hours of filtration were successful.

To identify the thermal/chemical stability of the PRD-66 material, W-STC subjected 10" mini-candles to 400 hours at 870°C, in a 5-7% steam/air environment at 1 Atm. Additional samples were subjected to 400 hours at 870°C, in a 20ppm NaCl/5-7% steam/air environment at 1 Atm. X-ray diffraction was used to compare the crystalline compositions of the materials. Neither of the test conditions had any measurable effect on the PRD-66 material.<sup>3</sup>

#### **3.3.1 Tidd Test Segment 4**

After the testing at Westinghouse, three PRD-66 candle filters were placed into field testing at American Electric Power's Tidd Pressurized fluidized bed combustor (PFBC) filter vessel. The PRD-66 candles were placed in the middle array of the vessel. They were exposed to temperatures up to 760°C and operated for the entire duration of the test segment, 1700 hours with ash loading of 3200 ppmw. All three of the PRD-66 filters survived the test segment and suffered no damage. Upon inspection of the filters after exposure, only a loose, thin (approximately 1/8" thick) ashcake clung to the candles. Despite significant ash bridging problems in the test, no ash bridges were found on the PRD-66 candles. Mechanical property tests performed by Westinghouse on ring segments cut from the exposed filters showed no decrease in mechanical properties after the 1700-hour exposure. The only significant negative finding in the test was that the wall of the PRD-66 filters had become filled with trapped ash. At the time, this was attributed to ash penetration from the inside of the filter, due to ash reaching the "clean side" of the filter vessel from other broken candle filters tested in the same plenum.<sup>2,3</sup>

From the results of this test segment, DLC concluded that PRD-66 candle filters were resistant to attack by the corrosive atmosphere resulting from coal combustion. Further, it was concluded that PRD-66 filters had the necessary mechanical strength to survive filtration and backpulse cleaning for at least 1700 hours of operation. The complete retention of mechanical properties in post-exposure testing suggests that under the conditions in Tidd Test Segment 4, significantly longer useful lives would be possible.

### **3.3.2 Tidd Test Segment 5**

Concurrent with the development of the low-pressure and dual-membrane filter elements under this program, twenty-two "baseline" PRD-66 candle filters (identical to those used in Test Segment 4) were placed in service in Tidd Test Segment 5. After the test, it was discovered that all of the PRD-66 candle filters had experienced significant damage. Two types of failure were observed. The first was a classic flange failure, with filters broken in the holder area where the flange transitions to the filter body. The second failure mode was observed mid-body, with approximately half the filter body remaining intact. In this failure mode, "divots" were taken out of the filter body, appearing as lenticular avulsions greater than a millimeter deep, as shown in Figure 14. In filters with mid-body failures, fracture occurred at these thinned spots in the body wall, often where a "divot-in-a-divot" had removed most of the wall thickness.<sup>2,8</sup>

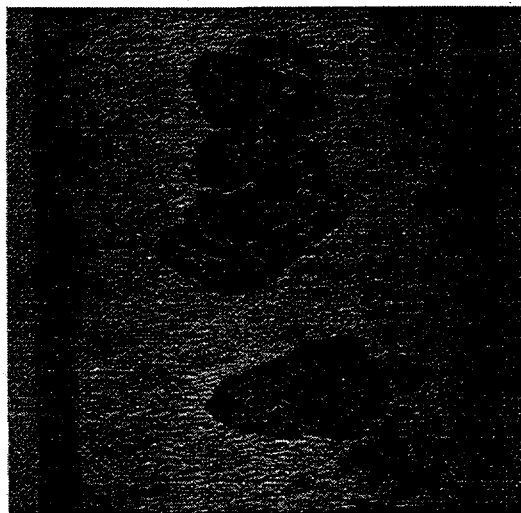


**Figure 14 - "Divots" in PRD-66 filter tested in Tidd Test Segment 5.**

### **3.3.3 Analysis of Field Exposed Elements (Subtask 3.4)**

To understand the cause of the discrepancy between the results of Tidd Test Segments 4 and 5, DLC undertook Task 3.4 of this program, entitled "Analysis of Field Exposed Filters". This task

was carried out in five phases: Consultation, Elimination of Known Faults, Hypothesis Formulation, Hypothesis Verification, and Correction.<sup>8</sup>

*3.3.3.1 Phase 1 - Consultation*

In the Consultation phase, DLC held discussions with numerous experts in the field of hot gas filtration, including Ted McMahon, Rich Dennis and Dwayne Smith of FETC, Mary Anne Alvin and Rich Newby of Westinghouse Science and Technology Center, Tina Watne and John Holmes of the University of North Dakota's Energy and Environmental Research Center, and Dick Tressler of Penn State. Valuable evidence and insight was gained from these discussions, which is incorporated into following summary.

*3.3.3.2 Phase 2 - Elimination of Known Faults*

In Phase 2, DLC undertook detailed evaluations of all the manufacturing records for filters supplied to Tidd Test Segment 5 to seek any anomalies in manufacturing which might explain the differences in performance. While some minor changes in the process were found, no process variations correlated with performance. X-ray diffraction tests on the filters fired in the same run with Test Segment 5 filters showed no difference with those in Test Segment 4.

*3.3.3.3 Phase 3 - Hypothesis Formulation*

Unable to find any significant differences in the filters, Phase 3 focused on physical evidence found in filters which survived Test Segment 5 in whole or in part, and documented differences in run conditions between Test Segments 4 and 5. As shown in Table 4, there were significant differences between Test Segments 4 and 5.

Test Segment	Tidd 4	Tidd 5
Test Duration	1700 hrs.	1100 hrs.
Survival Rate	100%	10%
Ash Cake	Thin, uniform	Thin, patchy
Damage	None	Divots, mid-body Broken, flange
Bridging	None	None
Operating Temperature	660 - 760°C	760 - 845°C
Ash Loading	3,200 ppmw	18,000 ppmw
Primary Cyclone	De-tuned	Inactive

**Table 4 - Comparison of test conditions in Tidd Test Segments 4 and 5.**

Ash loading increased from 3,200 ppmw to 18,000 ppmw because of the inactivation of the primary cyclone upstream of the filter vessel. The mean particle size of the ash increased significantly. The highest run temperature increased from 760 to 845°C. Different adsorbents and coals were used. In Test Segment 4, the PRD-66 candle filters were placed in the middle array, while in Test Segment 5, they were in the top array. Two failure modes were observed. One was a classic flange failure, with the fracture locus high up in the holder. These filters, in order to remain identical to the ones tested in Test Segment 4, did not use the selective reinforcement of the flange area described in Section 3.2.4. This reinforcement technique would have increased the strength of the PRD-66 material by about 50%. A second, more puzzling failure, was that found in along the body of the filters. The physical evidence seen on the filters included "divots", as shown in Figure 14.

"Divots" are pieces of the candle filter membrane and body, avulsed from the filter. Such "divots" were found aligned along the filter body on roughly opposite sides. A "divot" was also found under the sock and holder, which eliminates mechanical impact as a cause of the damage. There was no visible evidence of corrosion. The filter body walls were filled with ash, as they had been in Test Segment 4. The body of the filter was covered with a thin layer of loose ash, roughly 2mm thick in most regions. There were also denser ash deposits, aligned with the "divots" described above. All "divots" were packed with dense ash, though some ash-packed "divots" were covered with loose ash. Finally, in Test Segment 5, all filters of all types in the top array were somehow "glued" in place (strongly adhered to their holders). This was not observed in the middle or bottom arrays. Filter segments tested by Westinghouse showed no decrease in mechanical properties after exposure. Finally, micrographs taken at EERC by Tina Watne showed inclusions of a white material, identified by EDX as containing magnesium, calcium, sulfur, and oxygen, well inside the filter body, see Figure 15. This white deposit was of a physical size far too large to have penetrated the undamaged filter above it intact. Undamaged filter areas showed no such deposits.

Based on this evidence, a hypothesis of the failure mechanism of PRD-66 candle filters in Test Segment 5 was formulated. Despite earlier results of room temperature and high temperature tests to the contrary, ash that contained adsorbent penetrated the surface membrane of the PRD-66 filters. This ash then became trapped in the bulk filtering body of the candle. Once trapped there, it was subjected to long term exposure of hot SO<sub>2</sub> gas, causing in situ sulfation of the ash to calcium and/or magnesium sulfates in the pores and microcracks of the filters.

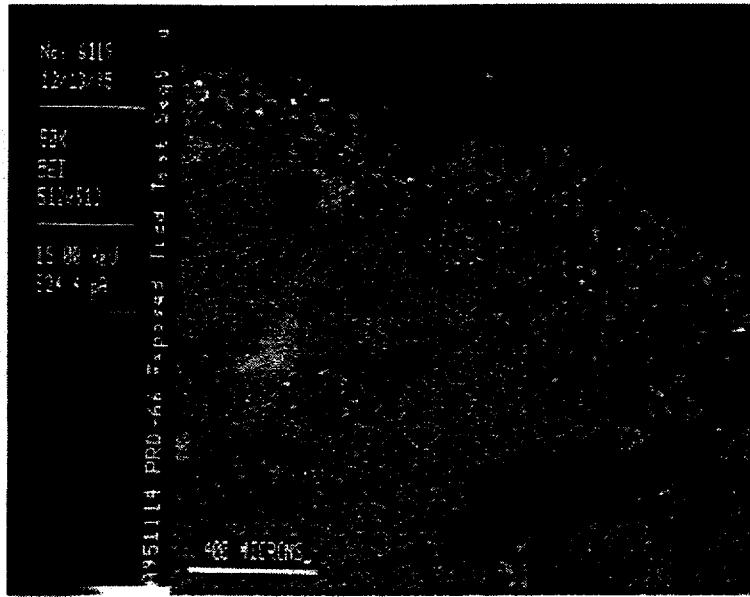


Figure 15 - White deposit (middle left) in vicinity of "divot" (upper right).

Once lodged in a microcrack at high temperature, these deposits could change in size by several mechanisms. One possible damage mechanism is by thermal expansion and contraction of the sulfate deposit during process interruptions, of which there were several in Test Segment 5. A second possible mechanism is by crystal growth from the hydration of sulfates during cooling in a moisture-containing atmosphere, which also would occur on process interruptions. Figure 16 shows how the unit-cell volume of anhydrous magnesium sulfate increases as it picks up waters of hydration.

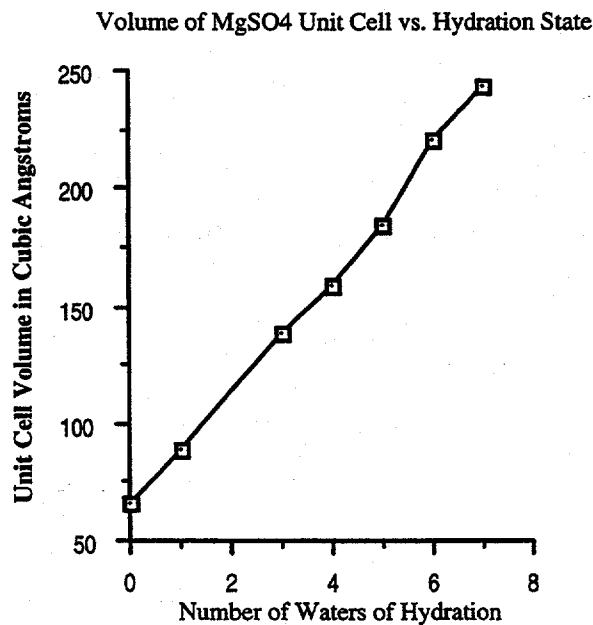


Figure 16 - Unit-cell size of magnesium sulfate versus state of hydration.

The roughly four-fold volume increase associated with formation of the hexahydrate salt would induce a linear strain in a microcrack of over 150%, far larger than the strain tolerance of most ceramics. By either of these mechanisms, severe internal stresses could be placed on the filter body, causing localized failure near a sulfate deposit. In areas where multiple deposits formed, a "divot-in-a-divot" could occur, either fracturing the wall or weakening the wall enough to cause mechanical failure during a backpulse.

#### *3.3.3.4 Phase 4 - Hypothesis Verification*

In Phase 4, DLC set out to verify that 1) this hypothesis is in keeping with the known conditions of Test Segment 5, and 2) the possibility of penetration of ash through the surface membrane, contrary to previous test results. DLC found that all conditions necessary for the hypothesis to be true existed in the Tidd test conditions. All that was required was the presence of trapped ash in the filter, the presence of gas phase SO<sub>2</sub>, and moisture, plus rapid temperature excursions. All these circumstances can be verified from knowledge of the system, the run history, and physical examination of the field exposed filters. To verify that it was possible that ash leaked through what was thought to be 'leak proof' surface membrane, DLC devised a room-temperature test of surface filtration characteristics more rigorous than the ones it had previously passed. In the previous tests, filter segments were exposed to gas flows containing ash. Once a smooth filter cake built up, it was supposed that the ashcake would strongly adhere and then take over filtration. A sample passes the test if no ash penetrates to the inner diameter. Since physical evidence from Tidd Test Segments 4 and 5 showed that the ashcake was thin and only loosely adhered, DLC worked under the assumption that the surface of the PRD-66 filters released the ash essentially completely on each backpulse. To mimic this ash removal in DLC's laboratory, after exposing filter segments to ash by applying a vacuum to the inner diameter, the resulting ashcake was physically removed with light brushing. This ash exposure/cleaning cycle was repeated 25 times. The intent was to simulate the effect of complete ashcake release after a series of cleaning backpulses. Figure 17 illustrates the apparatus used to conduct this test.

In this test, ash consistently penetrated the membrane of the "baseline" filter and accumulated in the filter wall. Figure 18 shows an example of a 2"-segment, exposed to 25 PIT cycles, viewed with transmitted light; the light source had been inserted into the sample and the examination was performed in a darkened room.

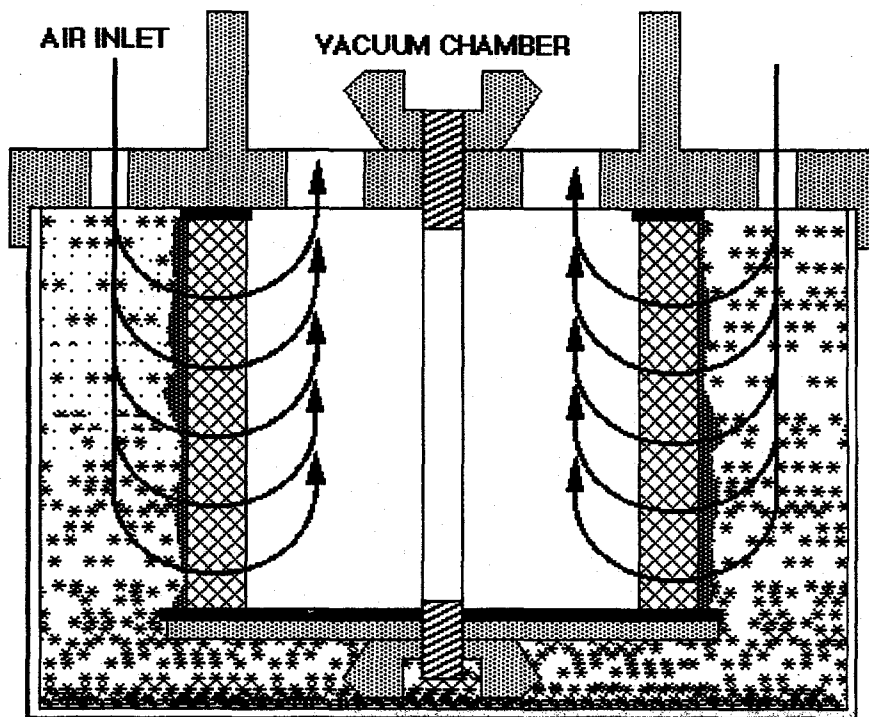


Figure 17 - Particle Infiltration Test (PIT) Device



Figure 18 - PIT-exposed sample viewed in transmitted light.

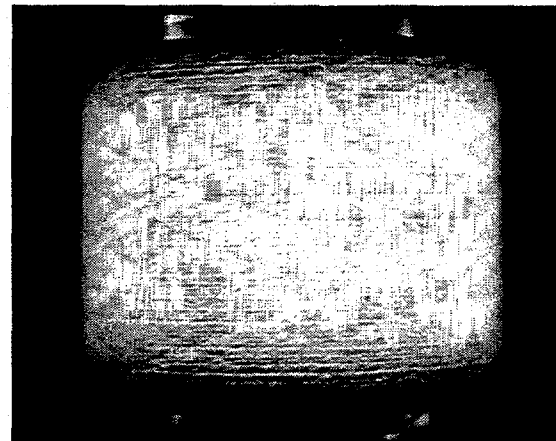
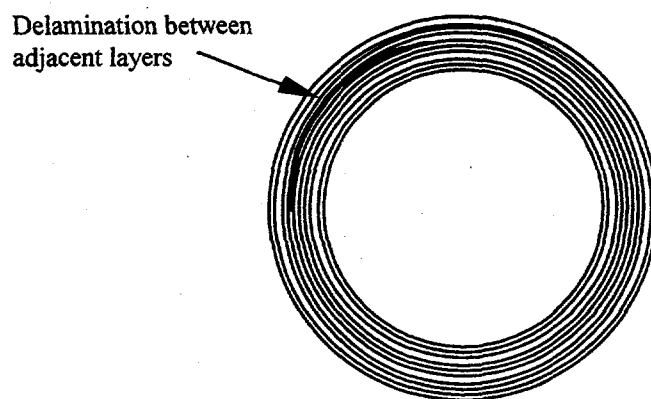


Figure 19 - Untested sample viewed in transmitted light.

When compared to an untested filter segment (Figure 19), areas of ash infiltration appear as dark streaks and spots; in the case of the "baseline" membrane, these areas are many and widespread. Even after the extensive penetration shown in the figure, however, ash still did not penetrate to the inner diameter after 25 cycles. This indicates that the bulk filtering body does trap ash in the wall. Because of the expense associated with recreating the in-situ sulfation of the penetrated ash, no such experiments were conducted.

Further verification of this hypothesis was found by Westinghouse's independent investigation of the failure mechanism. Westinghouse discovered differences in the ash adhered to the filters and uncleaned surfaces in the top array, versus the ash in the two lower arrays. They verified that the filters of the top array were 'glued' in place. Westinghouse also reported the presence of magnesium sulfate hexahydrate in the ash, as found by X-ray diffraction, on uncleaned, stagnant surfaces of the top array, such as the holders and tubesheet. As described above, DLC hypothesized the formation of magnesium sulfate hexahydrate in the filter body as a potential cause of damage, without formally verifying the existence of the compound by XRD. Westinghouse's proof of the formation of the hexahydrate salt verifies that actual system conditions present in Test Segment 5 could cause its formation, and therefore supports the likelihood of DLC's hypothesis. The fact that no such compound was found in the middle array could explain why ash-filled PRD-66 candles in the middle array of Test Segment 4 showed no damage.

The presence of factors that may have contributed to the formation of "divots" was confirmed, but this theory alone could not explain the presence of "divots" in localized areas. The PIT evaluation indicated that ash penetration would occur in over half of the filter surface and examination of the exposed filters showed that the ash was thoroughly imbedded throughout the wall of the entire unit. As a percentage of the outside diameter, the "divots" would account for less than 5% of the surface. A significant contributing factor may have been the presence of regions, within the wall, of poor interlaminar strength. When a PRD-66 candle filter is cut into rings, it is common to observe regions where adjacent layers of yarn have separated from each other, as shown in Figure 20. Occasionally, these defects might extend approximately a quarter of the way around the circumference, and continue for 1-2" inches along the length of the filter element. They have been observed at random depths and positions within the support body and could never be correlated with any process variables.



**Figure 20 - Exaggerated illustration of a PRD-66 delamination**

It is possible that the "divots" were caused by the combined presence of three things: an environment conducive to sulfate formation and hydration, ash entrainment, and localized interlaminar weaknesses. Since DLC has no control over the PFBC environment, corrective action was focused on improving the surface filtration quality of the membrane and reducing the presence of delaminating within the support wall.

#### *3.3.3.5 Phase 5 - Correction*

The composition of the "baseline" slurry was fumed alumina, calcined A-17-grade alumina, and deionized water. Observations made during Subtask 3.1 suggested the resulting alumina matrix might not have had adequate bonding strength. It was also noted that in the green state (dried, but not fired), bonds between coated filaments could be damaged when removing the filter from the mandrel. An alternate composition was evaluated in which the fumed alumina in the slurry was replaced by aluminum chlorohydrate, as an alumina precursor. This ingredient imparts significant "green strength", unfortunately environmental controls were necessary to deal with the evolution of HCl that results during heating. To remove this hazardous byproduct from the effluent stream, an HCl scrubber was installed and tied-in to a furnace capable of heating to 800°C (the "low-fire" step), under Subtask 3.5. With the use of this new slurry, virtually no delaminations were apparent within the wall of the filter elements, fewer candles were damaged during mandrel removal, and better adhesion between adjacent yarns was observed.

With regard to the membrane quality issue, Westinghouse's filtration efficiency test exposed the filter to only one ash penetration challenge, and showed no penetration to the inner body. The test protocol assumed that once a smooth ash layer was built up, it would adhere to the filter surface, and thereby take over future surface filtration. The thin, loose ash cakes on PRD-66 filters after Tidd exposures, however, brought that assumption into question. The Westinghouse test protocol also assumed that if ash penetrated the surface membrane, it would immediately show up on the inner diameter. Based on the hypothesis described above, the standards by which a membrane is deemed "acceptable" needed to be changed, at least where PRD-66 was concerned. The PRD-66 membrane would need to function as a much better ash barrier to minimize the risk of "divots" and to reduce the pressure buildup caused by accumulated entrained ash.

For the "baseline" filter, the leakage through the outer membrane appeared to occur through tiny gaps between the adjacent yarns of the "wound-on" membrane. Apparently, the alumina slurry coating on the fiberglass yarns did not consistently bridge the gaps between the yarns and an

incomplete membrane formed. Furthermore, gaps appear to occur more frequently, where the membrane yarn covers a primary crossover point in the pattern of the support winding underneath.

Several options were evaluated for improving the quality of the membrane layer

1. a different filament winding pattern for the body
2. a double outer membrane
3. a different type of membrane yarn
4. additions to the membrane layer

To test the efficiency of such alternate membrane technologies, 2-inch test segments were exposed to the Particle Infiltration Test (PIT), described in Figure 17. All samples were examined in transmitted light for areas of ash penetration; a subjective scale of appearance, ranking from "1" (many large wide-spread infiltration areas) to "10" (no detectable areas of ash infiltration), was established. Several specimens of each candidate were generally prepared to evaluate reproducibility.

Another critical aspect of the evaluation was to quantify the backpressure of the experimental membranes. 8-inch specimens of the promising candidates were prepared. Many of the membranes, which were studied, had excellent PIT ratings, but resulted in backpressure above Westinghouse's acceptable limits. For 8-inch long units, tested at 5 scfm, the target was 10 inches water gauge. In some cases, new membranes were evaluated for permeability first; only acceptable candidates were leak tested in the PIT.

Almost one hundred different combinations of the variables mentioned above were tested. A statistical evaluation was not feasible, however, certain conclusions, concerning the effectiveness of the varying approaches, could be drawn.

Filament Winding Patterns. It had been observed that many gaps occurred where the membrane yarn covered a primary crossover point in the pattern of the support winding underneath. Attempts were made to alter the winding pattern of the body to create a smoother surface on which to wind the membrane yarn. Although initial changes looked promising, each new pattern was very time-consuming to model and implement, and produced only marginal improvements. Consequently, no changes were made to the "baseline" winding pattern.

Double Outer Wound Membrane. The addition of a second layer of membrane yarn, on top of the first, was evaluated using a variety of slurry types, yarn spacings, and yarn types. Although several combinations produced units with good PIT ratings, the backpressure exceeded the 10-iwg

target. Consequently, the winding of two outer layers of membrane yarn was not incorporated into the "baseline" product.

Different Membrane Yarns. PRD-66 filters use fiberglass yarn, which is available with varying amounts of twist. It was hoped that by using a less twisted grade, the yarn would lie flatter on the surface of the filter body, the edges of adjacent yarns could overlap, and the gaps could be eliminated. Although this concept was demonstrated, the untwisted yarn was very difficult to work with and broke frequently during winding. Consequently, no yarn changes were incorporated into the "baseline" product.

Additions to the Wound Membrane Layer. Initially, the focus was on filling the gaps between adjacent membrane yarns with ceramic fibers, ceramic particles or ceramic precursors. Although many combinations were effective filters, they had poor permeability (high backpressure). By using these filler materials *INSTEAD OF* a hoop-wound membrane yarn, permeabilities that are more reasonable were achieved. The contours on the surface of the filter body, however, made reproducibility difficult. The most effective solution was to apply a hoop-wound membrane with intentional gaps between adjacent yarns and then fill those gaps with a material that gave appropriate filtration and backpressure. This membrane modification was incorporated into the "baseline" product and was commonly referred to as a "combination" membrane.

In summary, to correct the problem of the leaky membrane, identified in Subtask 3.4, the most promising approach chosen for further study was a membrane comprised of a "hoop-wound" yarn with a ceramic filler material in-between adjacent windings. To improve the interlaminar strength of the support body underneath, the filter would be fabricated using the modified slurry composition.

### **3.4 Development of High Efficiency Membrane**

To facilitate this addition of a ceramic filler material, a new pattern was chosen for the 'hoop-wound' yarns allowing broader spacing between adjacent yarns. Instead of relying on the microcracks in the alumina slurry to provide adequate filtration, a more controlled material would be used to fill in the gaps and provide a uniform porosity. The approximate relationship of this new spacing to the original membrane spacing is depicted in Figure 21 and Figure 22, showing the additional filler material between the 'wound-on' yarns, and the additional membrane area created in this process.

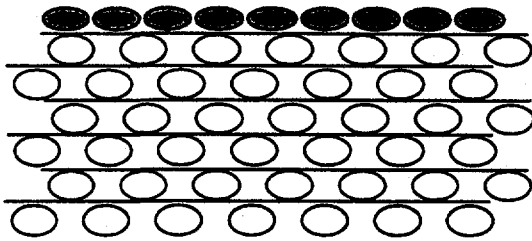


Figure 21 - Original wound membrane (wall cross-section).

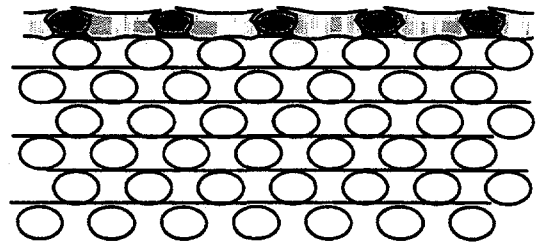


Figure 22 - Membrane with added filler (wall cross-section)

The composition of the filler material was varied over as wide a range of options and a variety of application techniques were attempted. Some of the variables evaluated included:

1. Particulate Alumina: 220-grit, 320-grit, 400-grit, 100-grit tabular alumina, fumed alumina
2. Ceramic Precursors: aluminum chlorohydrate, colloidal alumina, colloidal silica
3. Application Technique: brushing, hand-rubbing, spraying, immersion, squeegeeing
4. State of Filter Body: unfired, partially-fired, fully-fired

The criteria used for comparison consisted of "ease of application", "uniformity", "reproducibility", "adherence", "permeability", and "filtration efficiency". Candidate membranes were selected for further evaluation only if they scored a PIT rating >"9" after 25 exposure cycles. Figure 23 illustrates a unit with a rating of "10". The specimen pictured in Figure 18 would be representative of a rating of "3".

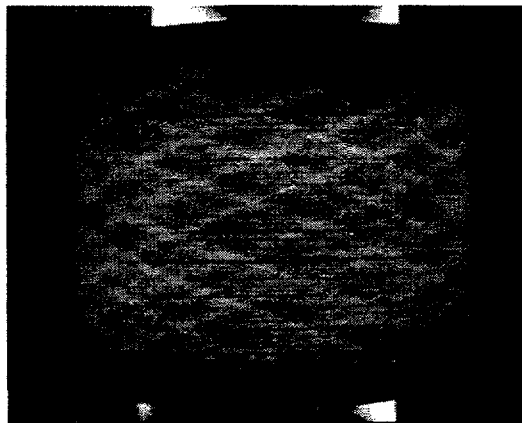
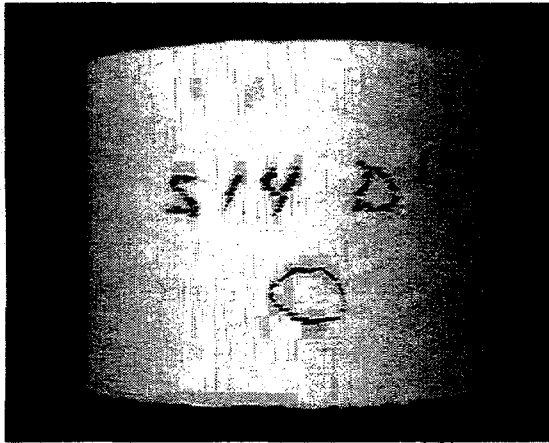


Figure 23 - Modified membrane with PIT rating of "10".

After assessment of a large number of filter segments, another advantage of transmitted light inspection became readily apparent. Any defects, which appeared as ash-infiltrated darkened areas in the PIT tested samples, had also been apparent in the untested samples when examined by transmitted light. Although small membrane defects on the order of 100-200 $\mu$  diameter were not readily apparent on routine visual inspection (Figure 24), they became visible as intensely bright points of light in

transmitted light inspection (Figure 25). Further, these defects were detectable in the filters prior to firing, allowing for the application of additional membrane filler before the final ceramic conversion firing.



**Figure 24 - Hole in membrane, undetectable under direct light.**



**Figure 25 - Hole in membrane, detectable under transmitted light.**

Controlled testing of specimens with membrane defects was conducted. Each sample was examined in transmitted light prior to firing, some pinholes were filled with additional material, and some were left open. Specimens were subjected to 25 PIT cycles. All sites where ash penetration occurred, during PIT exposure, had been easily located prior to firing. None of the filled pinholes showed signs of leakage. No additional defects developed during the final ceramic conversion firing. Figure 26 shows the result of testing a defective segment where a pinhole, detected prior to firing, was allowed to remain.

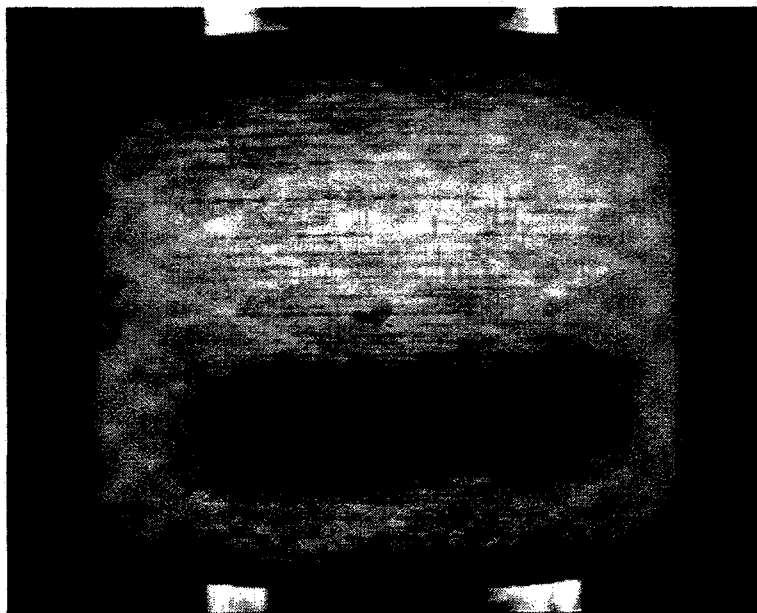


**Figure 26 - Hole in membrane after 25 PIT cycles, viewed in transmitted light.**

This defect was virtually undetectable when examined in direct light, but immediately obvious in transmitted light. This test and defect elimination procedure was added to DLC's standard manufacturing protocol for 100% of PRD-66 production filters.

From the many candidate membranes tested, two variants were selected for further evaluation. PRD-66M and PRD-66C were selected for their excellent, but different, combinations of filtration performance and flow resistance characteristics. Both of these membrane candidates were processed into full size filter elements for testing at the Westinghouse HTHP facility. PRD-66M has a mean pore size for filtration of about  $10.5\mu$  (Figure 27) with flow resistance comparable to the close wound membrane filters. Flow resistance of 1.5-meter filters was tested both before and after HTHP testing, as shown in Figure 28.

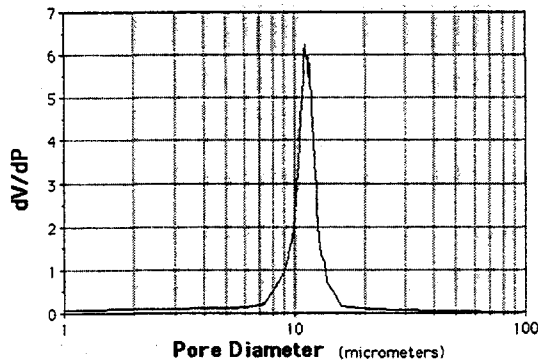


Figure 27 - PRD-66M membrane, measured pore distribution.

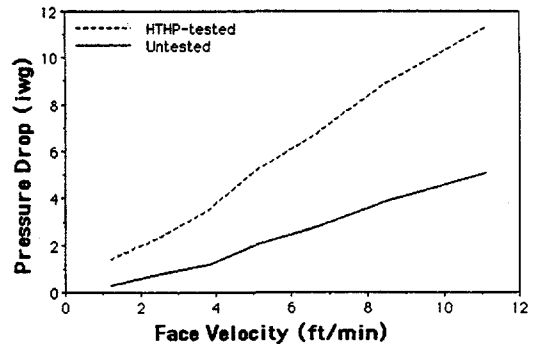


Figure 28 - PRD-66M flow resistance for 1.5-meter candles.

The second membrane candidate, PRD-66C, was chosen because of its unusually low flow resistance in combination with excellent filtration performance. With a mean pore size of about  $25\mu$  (Figure 29) its flow resistance is less than half that of filters with PRD-66M membranes (Figure 30).

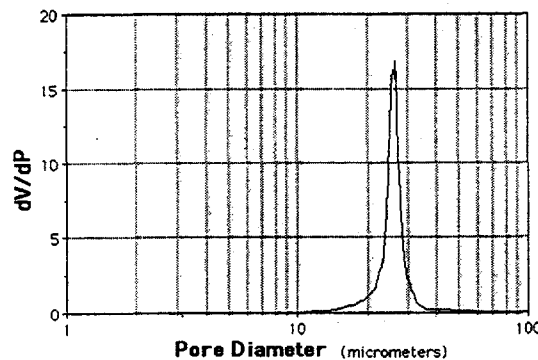


Figure 29 - PRD-66C membrane, measured pore distribution.

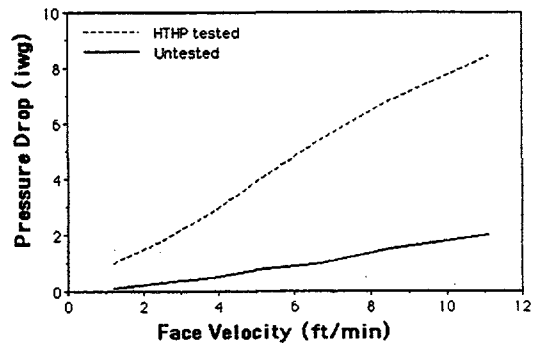


Figure 30 - PRD-66C flow resistance for 1.5-meter candles.

Both membrane types are considered viable candidates for future commercialization. The choice of which to use would depend on system requirements. Further refinements of the membrane composition are detailed in Section 3.5.3.2 "Variables".

### **3.5 Manufacturing Hot Gas Filters (Task 4)**

The focus of Task 4 was to lay the foundation for the repeat manufacturing of PRD-66 Hot Gas Candle Filters. The effort was divided into six areas: raw materials plan, process instrumentation, process variable experiments, process capability demonstration, equipment analysis and improvement, and evaluation of long-term degradation.

#### **3.5.1 Raw Materials Plan (Subtask 4.1)**

Discussions were held with DLC's quality organization to align the PRD-66 product with the company's overall quality plan. Copies of DLC's documentation requirements for raw materials specifications are detailed in Appendix 1. DLC will develop specifications for all raw ingredients necessary to the production of PRD-66 Hot Gas Candle Filters and require Certificates of Conformance (COC) and/or Certificates of Analysis (COA) with each shipment which document conformance of the incoming raw ingredients with specifications. Raw material suppliers were contacted about our requirements and were very cooperative in meeting them.

#### **3.5.2 Process Instrumentation (Subtask 4.2)**

The goal of this effort was to identify any critical equipment used to perform in-process measurements and establish methods to assure the level of calibration necessary to maintain process control.

The most important instruments used in fabricating hot gas candle filters are the electronic balances. Several balances, with different accuracy ranges, are utilized at different stages of the process. When winding candle filters, the bobbins of feed yarn (see Figure 1) are positioned on balances, which have a maximum load of 2,000 grams (+/-0.1 gram). The amount of yarn that is used in the preform is determined by the net change in the indicated weight of the feed bobbin. This weight, when compared to the weight of the actual candle, is used to calculate the amount of alumina

picked-up when the yarn is dipped into the alumina slurry (see Figure 1). Adequate pickup is necessary to insure the strength of the product.

A larger capacity balance, with a +/- 5-gram readout, is necessary for weighing the raw materials that comprise the alumina slurry. This balance is also used for the weighing of the candle filters; although, a more accurate balance with +/- 1-gram accuracy would be preferable for this purpose, if one was available.

All balances are calibrated annually in accordance with NIST HB44, ISO 10012-1 and ANSI/NCSL Z540 requirements. During the period of this contract, balances were calibrated several times and all were found to be within acceptable tolerances.

The only other critical instrument used in the PRD-66 process is a Brookfield viscometer. This device measures the viscosity (resistance-to-flow) of liquids. Viscosity standards were purchased from Brookfield with known viscosities similar to that of the alumina slurry used in the PRD-66 process. No measurable deviations from calibration were observed throughout the period of this contract.

Although the viscosity of the slurry is critical in a broad sense, experiments performed during Task 4.3 (3.5.3 - Process Variables Experiments) indicate that variations as high as 50% from nominal have no impact on the process. For this reason, the viscometer does not require routine calibration checks. It is critical, however, to ensure that the settings on the instrument are always appropriate for the spindle being used. An incorrect setting, for example, could lead one to believe that the viscosity is 100 cps, when in fact it is 1,000 cps. For this reason, use of this equipment is restricted to the PRD-66 project staff, and is used only for alumina slurries having similar viscosities.

### *3.5.3 Process Variables Experiments (Subtask 4.3)*

The focus of this subtask was to identify critical process parameters and vary them systematically to learn their effect on the product. In order to identify which variables the process was most sensitive to, ranges were chosen to encompass and exceed the existing specifications. If there was minimal sensitivity at the values tested, the existing specifications would be deemed acceptable. If sensitivity was detected, a more thorough evaluation would be conducted in order to define appropriate parameter limits.

The standard conditions for winding the fiberglass yarn included the use of the improved slurry composition, which had improved strength in the dry-state and better interlaminar adhesion, see Section 3.3.3.5.

### 3.5.3.1 Variables Impacting the Support Winding

The variables studied for their impact on the winding of the filter support were slurry viscosity, winding speed and atmospheric humidity. The ranges investigated were chosen based on current process capability to control them, see Table 5.

Variable	Lower Limit	Upper Limit
Winding Speed	- 22%	+ 22%
Alumina Slurry Viscosity	- 50%	+ 50%
Relative Humidity	20%	80%

Table 5 - Process variables investigated for winding filter support.

Candle filter support structures were wound, without flanges and without membranes. Winding was terminated when the weight of the fiber wound reached 1100 grams. Any unusual events that occurred were noted during the course of each run. After overnight air drying, tubes were each cut into eight, 8" long sections and the two end pieces retained as scrap. All portions were fired to 700° C ("low-fired"), held for one hour and allowed to cool to room temperature. All portions were weighed and measured, then high-fired to approximately 1400°C. Alumina pickup was calculated based on the low-fired weights and the known weight of the fiberglass yarn and high-fired materials were flow tested and inspected for delaminations. A summary of the results is depicted in Table 6.

Variable	Lower Limit	Upper Limit
Winding Speed	very slight increase in diameter	no detectable effect
Alumina Slurry Viscosity	statistically significant decrease in alumina pickup	no detectable effect
Relative Humidity	slight increase in diameter	slight decrease in diameter

Table 6 - Observed impact of process changes on support winding.

The lower and upper limits, which were tested, are all outside the normal process limits, yet, only the use of an "alumina slurry with half of the normal viscosity" resulted in a statistically significant change. No statistically significant variations in the product occurred within the nominal viscosity range. None of the other changes were statistically significant, suggesting that the normal process control limits are adequate for the reproducibility of PRD-66 candle filters.

Experiments were also conducted to determine the effect of "process interruptions during the winding operation" on process quality. The most critical type of interruption is an unattended yarn break during winding. To simulate this type of problem, the winding was intentionally stopped approximately half way into an otherwise routine winding run. The package was allowed to sit for approximately 15 minutes while still rotating, although a five-minute interruption would be more typical of current process norms. This experiment was conducted under a range of humidity conditions. Winding was restarted following standard procedures, and stopped at the target diameter. After the tube was dried overnight, it was cut, low-fired, weighed, and measured as described earlier; the specimens were then high-fired through a standard cycle to approximately 1400°C.

The only sample impacted by the winding interruption was the unit wound at the lowest humidity condition, which was outside of the normal operating range. When the completely fired material was cut, and the cross-section examined, a slight delamination could be discerned at approximately the mid-way point in wall, closely corresponding to the point at which the winding had been interrupted. Apparently, process interruptions of up to 15 minutes can be tolerated without adversely affecting the product, except in humidity conditions which are generally outside the normal range. Besides the resulting improvement in product yields, the insensitivity to interruptions will allow the use of "short bobbins" of fiberglass yarn. Standard bobbins of S-2 yarn typically have about 25% more yarn than is actually required for winding one candle filter. To stop the winding, and string-up a new bobbin of yarn usually takes approximately three minutes. The ability to do this without jeopardizing product quality will lead to less wasted yarn and lower costs.

An additional variable, which had to be added to this experiment, was the impact of fiberglass yarn "twisted" by a different company. Owens-Corning FiberGlas (supplier of S-2 glass yarn) decided that they would no longer directly supply yarn that is "twisted" in a wide assortment of configurations, including that required by this process. Two alternate sources of this twisted yarn were identified; only one, however, was reasonably priced. Three candle filters were fabricated from yarn twisted by the Varflex Corporation (Owens-Corning is still the sole manufacturer of the S-2 glass filaments). The run information was compared to the database that had been generated in earlier portions of this task. Evaluations were conducted on "alumina pickup", diameter growth

rates, frequency of yarn breaks, and integrity of the overall structure. The twisted yarn from Varflex appeared to be either equivalent or superior to the original material in all tests. DLC's current inventory of yarn (purchased from Owens-Corning) is adequate to complete the fabrication of candles required for this program, but future purchases will be made from Varflex.

### 3.5.3.2 Variables Impacting the Membrane

As discussed in Section 3.4 "Development of High Efficiency Membrane" several variables were identified as being critical to the formation of a satisfactory membrane for the PRD-66 Hot Gas Candle Filter. Under Task 4.3, extensive tests were conducted to identify a membrane-filler formulation that would consistently yield low backpressure units with good filtration. The variables explored included:

1. 4 different solid-to-liquid suspension ratios
2. applying the particulate material to low-fired or high-fired candles
3. 2 different particle or grit sizes of alumina
4. 2 different levels of a fusible binder addition

Evaluations of items "1" and "2" were based on subjective comparisons of the ease of preparation and application of the filler material. The preferable solid-to-liquid ratio (2:1) was an aqueous suspension with a consistency similar to very, smooth peanut butter. More consistent results were achieved by applying this filler material to the surface of low-fired candles. Samples prepared in this manner with the medium-grit membrane, however, frequently developed extremely fine cracks in the membrane during the final firing, visible only with intense scrutiny using transmitted light. These cracks were so fine that no TIDD ash penetrated after 25 PIT cycles. Evaluations of items "3" and "4" were conducted in a more quantitative fashion, as shown in Table 7.

Both the "coarse" and "medium" grit alumina particulate are capable of producing membranes with a PIT rating of "10". The two grit sizes, however, had different ashcake release characteristics in the PIT evaluation, with the ash being more adherent to the coarse-grit membrane. In the Karhula field trial, this type of candle exhibited the formation of a traditional "conditioned ash cake layer". Tests of the original "baseline" candle in TIDD did not form such a layer; the repeated exposure of the imperfect membrane surface, after backpulsing, was thought to have contributed to the entrainment of ash in the filter wall.

### PRD-66 Membrane Variations and Reproducibility

8" Unit ID	Full Length Candle ID#	Membrane Grit Size	wt% Binder	Weight of Added Membrane	Backpressure in-wg @5scfm
1	553	Medium	5%	9.03	5.6
2	553	Medium	5%	8.50	7.0
3	553	Medium	5%	8.55	5.6
4	553	Medium	5%	8.94	5.5
5	553	Coarse	5%	8.14	2.2
6	553	Coarse	5%	7.23	5.2
7	553	Coarse	5%	8.53	3.4
8	534	Coarse	5%	7.67	2.6
9	534	Coarse	5%	7.38	1.8
10	534	Medium	5%	7.85	4.0
11	555	Medium	5%	7.22	5.4
12	555	Medium	5%	7.85	5.6
13	534	Coarse	5%	5.73	3.0
14	555	Coarse	5%	5.83	1.9
15	555	Coarse	10%	-	2.1
16	555	Coarse	10%	-	3.2
17	555	Coarse	10%	-	3.1
18	555	Coarse	10%	-	1.9

**Table 7 - Impact of grit-size and binder content on backpressure.**

The data shown in Table 7 was also used to evaluate the impact of applying reproducible amounts of the particulate membrane. A correlation of the weight of the membrane filler and the backpressure was plotted in Figure 31. In general, the exact amount of the added membrane filler did not directly effect backpressure, at the quantities being used; in severe cases, however, excess material has been observed to crack during the high-fire step.

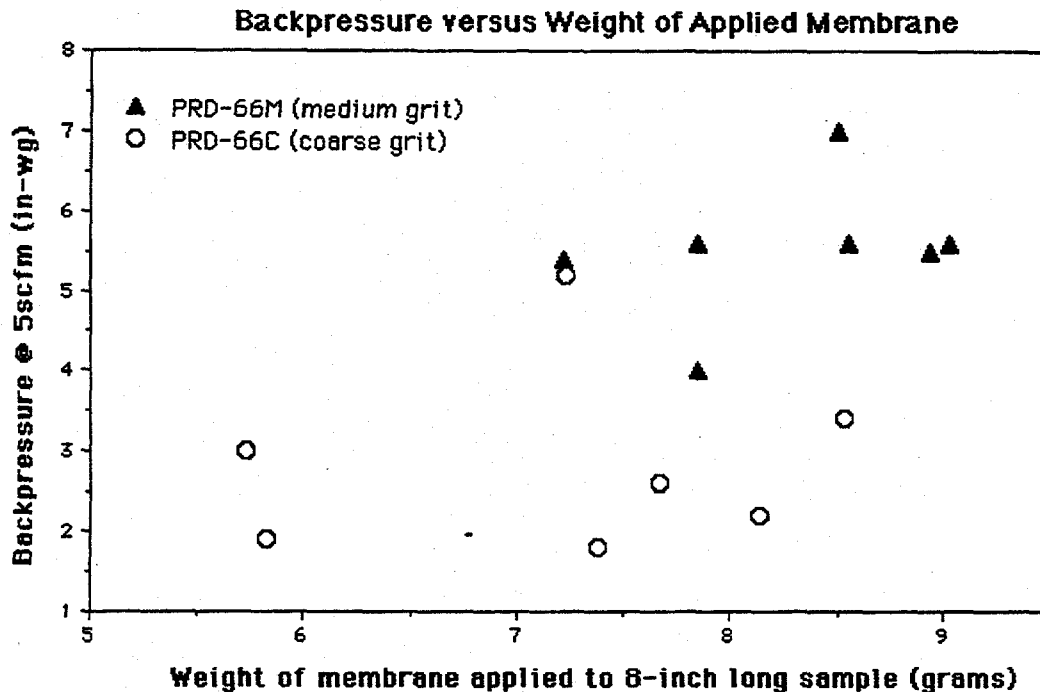


Figure 31 - Impact of membrane weight and type on backpressure.

Backpressure also appeared to be relatively unrelated to the binder content in the larger grit size composition, see Table 8. The higher level of fusible binder addition seemed to be preferable for the coarse-grit filler; the resultant material adhered better to the surface of the candle, as observed in the repeated brushing involved in the PIT evaluation. This level of fusible binder was not necessary with the medium-grit filler-material, probably because the higher surface area of the finer particles sintered more readily. Fortunately, a higher level of fusible binder did not seem to significantly impact backpressure.

**Backpressure of Coarse Samples Only vs. Binder Content**

Binder Content	No. of samples	Backpressure @ 5scfm (in-wg)	
		Average	Std. Dev.
5%	n=7	2.9	1.2
10%	n=4	2.6	0.7

Table 8 - Impact of binder content on backpressure of PRD-66C.

Based on the experiment described above the membrane formulations chosen for further evaluations were: "medium grit with 5% binder" and "coarse grit with 10% binder"

In addition to the membrane experiments described above, an evaluation was conducted to determine the effectiveness of filling "pin holes" in the unfired membrane. Eighteen low-fired, 8" filter segments were coated with either the "coarse" or "medium" grit membranes. After the membrane dried, each unit was checked with transmitted light for "pin holes". Additional membrane filler was then applied to those areas and marked with a high-temperature marking pencil, to make later identification possible. After high-firing, all specimens were examined again. All patched areas appeared completely sealed and no additional "pin holes" developed.

Earlier in this section, mention was made of the formation of extremely fine membrane cracks after high-firing the PRD-66M candle filters. The reason for their occurrence was not determined. In general, these flaws were only visible using transmitted light, and then, only if you knew exactly what to look for. If significant amounts of excess filler-material remained on the surface, the cracks were more severe and visible to the eye under normal lighting conditions. Preparation of multiple samples, from virtually identical tubes, has yielded significant information. Only the membrane made with the medium-grit, or finer, alumina particulate exhibits the problem, under normal conditions. The problem is minimized by using lower levels of the fusible binder addition, but not eliminated. When several 8" samples, from the same candle, were prepared in the same way with the medium-grit filler, and fired side-by-side, only one sample in the batch had cracks. As noted earlier, a specimen with a crack was PIT-tested with TIDD ash; the ash was trapped in the membrane and did not penetrate into the support wall. It is unknown whether or not this condition jeopardizes the successful operation of the candle. Aggressive investigation was discontinued due to the time constraint of providing filters to Westinghouse for testing. The best-known formulations and application methods would be used. General and specific information, with regard to handling of the candles, placement within the furnace, etc., would be monitored and correlations would be sought with any incidence of cracking.

#### *3.5.4 Process Capability Demonstration (Subtask 4.4)*

The focus of this subtask was to produce three batches of candle filters, according to the specifications required by the Westinghouse Advanced Particulate Filtration (APF) System, as shown in Figure 32. Each batch consisted of ten candles, manufactured under identical conditions. Before beginning each batch, critical components of the process equipment was inspected. Where feasible, new parts were put into service and process changes were incorporated to improve the product quality and process yields. An evaluation was conducted on all measurable features of the filters to

assess controllability and product uniformity. Significant aspects of the process, which effected final yields, were identified. Eight of the first-quality candles were used for high-temperature, high-pressure (HTHP) testing at Westinghouse Science and Technology Center (see Section 3.6.1). Twelve of the first-quality candles were field tested at the Foster Wheeler 10 MWt PCFBC facility in Karhula, Finland (see Section 3.6.2).

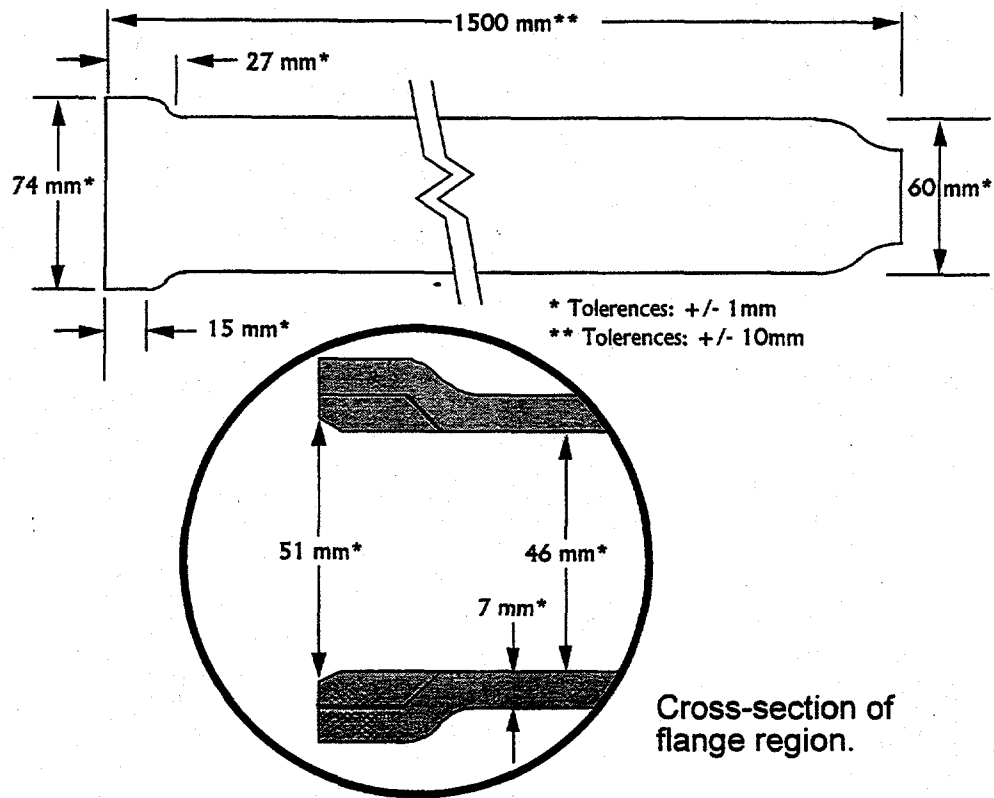


Figure 32 - PRD-66 Candle Filter dimensions

During this capability study, twenty-one good candles were produced, out of a possible 30, or 70% yield. Table 9 gives a detailed evaluation of all elements fabricated. Table 10 summarizes the data into the three, ten-unit runs, which were conducted.

Seven elements were rejected as a result of physical damage incurred during some stage of the processing. One element was rejected because the flange was out-of-spec (too long). One element was rejected for a poor quality membrane. Although, the "inside edge diameters" of nine flanges were out-of-spec, Westinghouse felt confident that their holder assembly could accommodate them, so they were not rejected.

PRD-66 Hot Gas Candle Filters											
<i>Process Capability Demonstration - 30 Candles</i>											
Candle	Weight (g)	Flange (mm)				Bend (mm)	Mem. Type	Backpressure (iwg@50scfm)	%Al <sub>2</sub> O <sub>3</sub> Pickup	Visual Exam	Pass/Fail
		OD	ID	Length (5)	Length (4)						
564	2610	73.3	50.7	27.0	15.5	2.0	M	7.4	55.9		
565	2575	73.1					M	6.8	56.5	bumped in mid-candle after winding	Fail
566	2600	73.4					C	2.8	55.7	bumped in mid-candle after winding	Fail
567	2505	73.6	51.5	27.1	15.3	1.0	M	6.0	55.0		P
568	2565	73.1	50.2	27.9	15.9	2.0	M	7.2	56.3		P
569	2520	73.2	50.3	26.8	15.7	0.5	M	7.9	56.0		P
570	2590	73.8	50.5	27.4	15.8	1.0	M	7.5	57.3		P
571	2540	73.2	50.3	27.3	15.8	1.0	C	3.6	56.0		P
572	2515	74.0	51.4	26.2	15.0	0.5	C	3.7	55.4		P
573	2485	74.0	50.6	26.6	14.7	1.5	C	2.1	54.9		P
574	2555	74.0	50.2	32.3	27.6	1.5	C	2.4	54.9	Flange cut too long	Fail
575	2555	73.4	53.5	26.1	14.1	2.0	C	5.1	56.6		P
576	2445	73.8	52.5	27.3	15.3	1.5	C	4.4	55.4	chip in memb. (7.5" from tip)	Fail
577	2495	73.2	52.9	27.4	15.4	0.0	C	4.3	56.0	finger prints	P
578	2365	74.2	52.0	26.7	14.7	0.5	C	3.2	53.5	chip in memb. (6.5" from flange)	Fail
579	2520	73.4	51.3	26.5	14.5	2.0	C	4.3	55.6		P
580	2570	73.0	50.5	27.5	15.5	0.0	C	4.2	56.4	poor bulk support wind pattern	P
581	2390	74.0	53.8	26.6	14.6	2.0	C	3.4	55.0	finger prints	P
582	2515	73.3	53.1	27.7	15.7	2.0	C	4.1	55.9	few scars, finger prints	P
583	2515	73.6	53.0	27.0	15.0	1.5	C	3.0	55.6	tip crack, fing. pr.	Fail
584	2550	74.0	53.3	27.6	15.6	2.0	C	4.1	56.6		P
585	2490	74.2	51.8	28.0	16.0	0.5	C	3.5	55.7	1/2" wide chip @ tip, finger prints	Fail
586	2555	73.1	51.8	27.7	15.7	1.0	C	5.2	56.6	large patches of excess memb. finger prints	P
587	2615	73.9	53.0	26.5	14.5	1.5	C	4.2	56.9	finger prints	P
588	2560	73.5	50.1	27.9	15.9	1.0	C	4.3	56.3		P
589	2595	73.9	51.1	27.6	15.6	2.0	C	3.3	56.6	chip in memb. (5.5" from flange)	Fail
590	2545	74.0	51.5	27.1	15.1	2.0	C	3.0	55.0	SEVERE support winding irregularities	Fail
591	2455	73.8	53.0	27.1	15.1	2.0	C	3.9	54.9	poor bulk support wind pattern, finger prints	P
594	2585	73.5	45.9*	26.8	14.8	2.5	C	3.0	56.6		P
595	2565	74.0	45.9*	27.9	15.9	2.5	C	4.0	56.7		P
Average	2522	73.7	52.1	27.5	15.8	1.5		3.7	56.6		
StDev.	60	0.4	1.2	1.1	2.4	0.7		0.8	0.8		
* at Westinghouse's request, the open end was not bevelled											
TYPE-C only											
Dimensions not detailed above											
				Ave.	StDev.					Ave.	StDev.
Overall Length				1502	2	Tube OD				59.7	0.3
Length of open filter				1417	7	Tube ID				45.8	0.2

Table 9 - Process Capability Demonstration

PRD-66 Hot Gas Candle Filters												
<i>Process Capability Demonstration - Summary</i>												
	Weight (g)	Length (mm)		Tube (mm)		Flange (mm)				Bend (mm)	Backpressure (iwg@50scfm)	%Al <sub>2</sub> O <sub>3</sub> Pickup
		Overall	Open*	OD	ID	OD	ID	L (5)	L (4)			
<b>TOTAL (30 candles)</b>											<b>TYPE-C only</b>	
Average	2522	1502	1417	59.7	45.8	73.7	52.1	27.5	15.8	1.5	3.7	56.6
StDev.	60	2	7	0.3	0.2	0.4	1.2	1.1	2.4	0.7	0.8	0.8
Target		1500		60.0	46.0	74.0	51.0	27.0	15.0	0.0		
Spec.		+/- 10		+/- 1.0	+/- 1.0	+/- 1.0	+/- 1.0	+/- 1.0	+/- 1.0	< 3.0		
<b>RUN 1 (10 candles)</b>												
Average	2551	1502	1405	59.6	46.0	73.5	50.7	27.0	15.5	1.2	3.1	55.9
StDev.	43	3	4	0.3	0.0	0.4	0.5	0.5	0.4	0.6	0.8	0.7
Max	2610	1505	1411	60.1	46.0	74.0	51.5	27.9	15.9	2.0	3.7	57.3
Min	2485	1499	1397	59.2	46.0	73.1	50.2	26.2	14.7	0.5	2.1	54.9
<b>RUN 2 (10 candles)</b>												
Average	2493	1501	1417	59.7	45.7	73.6	52.3	27.5	16.2	1.3	3.8	55.5
StDev.	70	3	6	0.3	0.2	0.4	1.2	1.8	4.0	0.8	0.8	0.9
Max	2570	1508	1426	60.0	46.0	74.2	53.8	32.3	27.6	2.0	5.1	56.6
Min	2365	1499	1405	59.3	45.5	73.0	50.2	26.1	14.1	0.0	2.4	53.5
<b>RUN 3 (10 candles)</b>												
Average	2552	1502	1418	59.8	45.9	73.8	52.0	27.4	15.4	1.7	3.9	56.2
StDev.	65	3	9	0.3	0.2	0.4	1.2	1.8	4.0	0.7	1.5	1.0
Max	2615	1505	1426	60.5	46.2	74.2	53.3	28.0	16.0	2.5	5.2	56.9
Min	2455	1500	1410	59.2	45.7	73.1	50.1	26.5	14.5	0.5	3.0	54.9

\* Open Length is defined as that portion of the filter which provides active filtration.

**Table 10 - Process Capability Summary**

The physical damage to the filter elements appeared to have two distinct sources. The first occasion for significant damage to occur was during the transfer of the developing candle from the bulk support winder to the membrane hoop winder (while it was still soft, damp and easily dented). Any obstructions on the equipment or between the winders increased the risk of damage. When two candles were dented, it was immediate and obvious.

Of more serious concern were several filter elements which each had a single chip (approximately 1/8"-1/4" long and 1/16"- 1/8" wide) in the membrane, discovered during final inspection. After final firing, the damaged areas "puckered" and the membrane easily flaked off when rubbed. Based on historical observations, the damage probably occurred while the candle was in the unfired or low-fired state. Possible causes include excessively tight gripping during a difficult mandrel removal or contact of the membrane with an inadequately padded area of the storage cart. In either case, damage would not have been apparent prior to the final high temperature firing.

Examining the standard deviation of the data, most of the features were within 3% of the average and within the acceptable range established by the Westinghouse protocols. The inside diameter of the flange and the length of the flange, however, were much more difficult to keep in-spec:

Inside diameter of the flange. The inside diameter of the flange was out-of-spec on 30% of the candles fabricated. The open end of each candle was finished-off by grinding a bevel on the inside edge, such that, the finished edge of the ID was 51mm +/- 1mm. The hand grinding technique, which was employed to create this bevel, was not adequately reproducible; machining was not a viable economic option. The original reason for the grinding was that the inside edge of the flange was occasional too friable, resulting in an irregular surface. Throughout the course of this program, however, with the adoption of the Chlorhydrol®-containing alumina slurry (see Section 3.3.3.5), the inside edge became much denser than with the original composition. The added step of grinding this area no longer appeared to be necessary; both DLC and Westinghouse agreed to eliminate this feature in future production runs.

Length of the flange. The data does not wholly reflect the difficulty encountered in meeting the required tolerances. Because the outside contour of the PRD-66 flange has no distinct edges, defining the precise location for cutting is not simple. It was also difficult to establish whether the flange was "in-spec" or "out-of-spec". All measurements were taken based on how the flange aligned with a plastic tool having a similar contour. Several candles which seemed to be slightly too long were hand-ground into spec. No problems were encountered, by Westinghouse or Foster Wheeler, mounting any of these candles for field trials. Eventually, better measurement techniques and better-defined specifications will be needed.

The data collected during the process capability run (see Table 9) indicated that the alumina matrix pickup varied from 53.5% to 57%. A possible link between diametrical compressive strength and alumina matrix pickup was investigated. 1" wide o-rings were cut from the candle with the 53.5% pickup and o-ring diametrical compressive tests were performed. The strength values were within the range of all measurements previously taken. During the course of Task 5 additional tests will be conducted on the candle with the lowest matrix, pickup to see if any impact on strength can be observed. Furthermore, any finished candle having a damaged portion, making it unsuitable for field use, will be cut up into 1" o-rings and tested in order to define the nominal strength range of PRD-66 filter elements. This information will be essential in determining if field-exposed elements are any stronger or weaker than the as-manufactured material.

An important objective of this task was to gain a better understanding of the process economics of manufacturing PRD-66 Hot Gas Filters. The most dramatic finding was that the utilization of the winding equipment was well below expectations due to the high level of equipment maintenance required. While some problems were anticipated as a result of wear, the biggest difficulties encountered were inherent in the basic winder design. Many of the features that make this device very versatile compromise its reliability under routine operating conditions. A simpler winder, designed specifically for PRD-66 candle filters, would require significantly less time, labor, and materials to maintain.

### *3.5.5 Equipment Analysis and Improvement (Subtask 4.5)*

During "Task 4.4 - Process Capability Demonstration", described in the previous section, an analysis of the rate of wear of critical components was conducted. Attention was initially focused on surfaces that were in contact with abrasive slurry-coated yarn and the moving components of the winder itself. As part of "Task 4.5 - Equipment Analysis and Improvement", the feasibility and cost of making improvements was evaluated and changes made where appropriate.

The first issue addressed was an increase in the frequency with which the slurry-coated yarn would break during the winding process. Breaks usually occurred when the traverse changed direction and the yarn needed to slide from one side of the guide to the other. The most obvious reason for this problem was that the alumina guide would develop grooves on either side, because of abrasion from the particulate alumina in the slurry. The deeper the grooves became the more likely the yarn was to break when the traverse changed direction. Two potentially more abrasion-resistant materials were evaluated: metal-matrix composite and polycrystalline diamond. The metal-matrix composite material turned out to be even more susceptible to abrasion. The polycrystalline diamond guide was never actually tried; it was prohibitively expensive to achieve a sufficiently rounded surface that would not cut the yarn. Since neither material offered any advantages over the high purity alumina, the alumina guide was changed out more frequently to keep yarn breaks to a minimum.

During this investigation, however, another reason for yarn breaks was observed. The yarn would most frequently break during the first 20 minutes of winding, when the guide changed direction at the tip-end of the mandrel. The mandrel on which the PRD-66 filter element was wound had a hemispherical shape at the tip end, going from 45 mm down to 6 mm in diameter in approximately 1" of length, as shown in Figure 33.

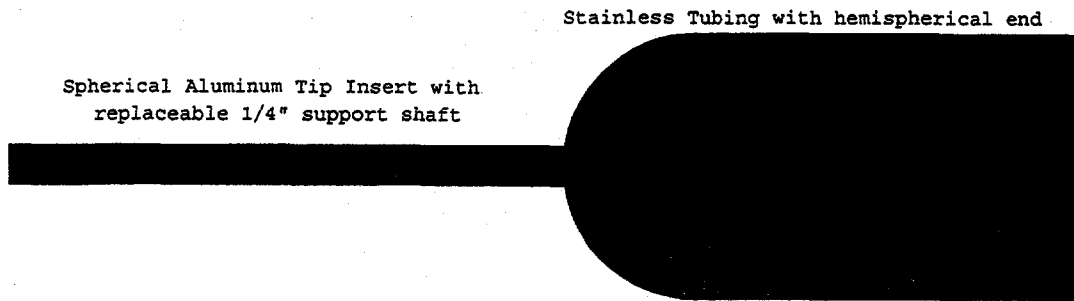


**Figure 33 - Tip of original steel mandrel**

When the yarn wound down to the narrow support shaft, the speed at which it was being removed from the yarn bobbin (see Figure 1) would slow dramatically; as the guide carried it back up to the 45 mm tubing, the yarn would be "tugged" suddenly, often breaking the yarn. As a layer of yarn accumulated on the shaft, thus increasing its diameter, this became less of a problem. During the first twenty minutes of winding, however, constant supervision and slower winding speeds were required. To address this problem a design change was made, to use a conical-shaped tip instead of a hemispherical one; this change was instituted along with other changes intended to create more easily removable mandrels. After the changes were implemented, the frequency of breaks dropped dramatically.

Another problem this task sought to address was the difficulty with which the wound filter was removed from the mandrel. In several cases, damage to the candle could result, which was not always easily detected until much later in processing (see Section 3.5.4). After unsuccessfully trying to find an outside vendor who could supply a mandrel that would meet DLC's needs, an in-house program was initiated. Several combinations of steel tubing, plastic tubing and rubber were evaluated. The mandrel chosen for future manufacturing use was made from readily available sizes of tubing, with a rubber conical tip, and could easily be removed from the filter after spending about 30 minutes in a freezer. Because of the use of standard tubing sizes, the filters were approximately 1 mm smaller in the inside diameter. Sample candles made on the prototype mandrel were sent to Westinghouse to determine if they anticipated any problems with the design. Westinghouse did have to modify the design of their "fail-safe devise" to accommodate the inside diameter change.

Another issue addressed in this task was the inadequacy of the procedure and tools used to cut the scrap ends from the dried candle filters. The standard procedure required the use of a razor knife, while rotating the candle (while still on the mandrel). After the finished candles were checked for perpendicularity, however, many flanges required hand grinding in order to meet the specification. A new concept was evaluated involving the use of a rotating, circular blade, while

rotating the candle/mandrel. A silicon carbide blade and a diamond wafering blade were both tested. The diamond blade was the most effective and was used with later candles made in the "Process Capability Demonstration". The need for hand finishing of the final filters was reduced.

A major equipment issue involved the repair of DLC's 15-ft long X 4-ft wide high-fire furnace. The deterioration of the roof insulation over the previous six years led to detectable temperature non-uniformities along the length. To compound this problem the furnace had to be relocated to a more suitable manufacturing area, this move caused additional damage to the roof insulation. Since there are no other furnaces readily accessible to DLC for firing 1.5-meter candle filters and the PRD-66 Hot Gas Filter Program was only user of this equipment, repairs were conducted under this program.

While some of these modifications were implemented during the "Process Capability Demonstration", all had been put in place by the start "Task 5 - Manufacturing 50 Candles".

### ***3.6 Field Testing of "Improved" PRD-66 Filter Elements***

#### ***3.6.1 High Temperature High Pressure (HTHP) Testing at W-STC***

Eight filter elements (four of each membrane type), manufactured during the first 10-candle run of the "process capability demonstration", were submitted to Westinghouse Science and Technology Center. Upon arrival, all candles were measured for room temperature gas flow resistance, as shown in Figure 34 and Figure 35. Both sets of filter elements met the W-STC tolerance of <1 in-wg/fpm for as-manufactured candles.

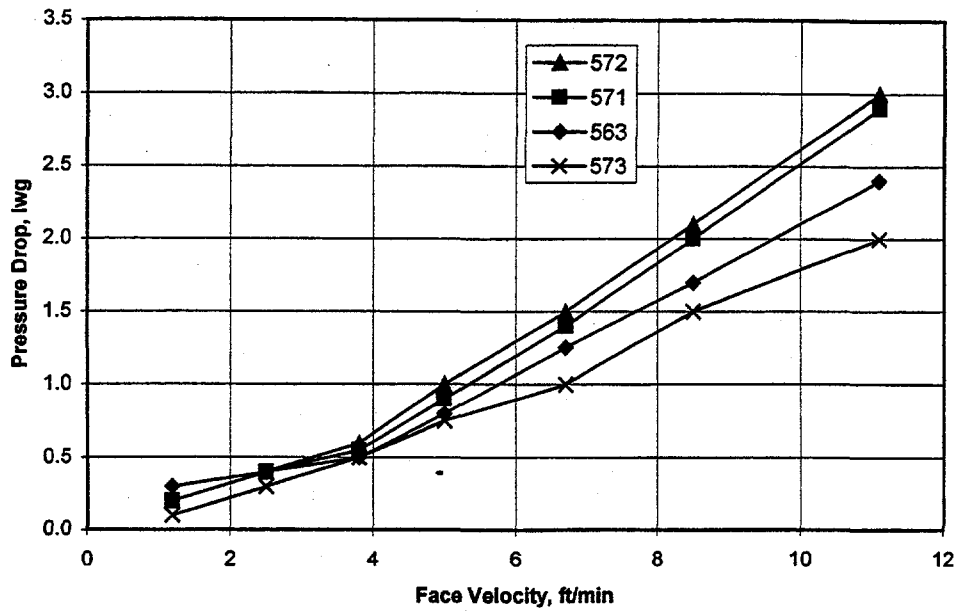


Figure 34 - PRD-66C - Room temperature gas flow resistance<sup>12</sup>

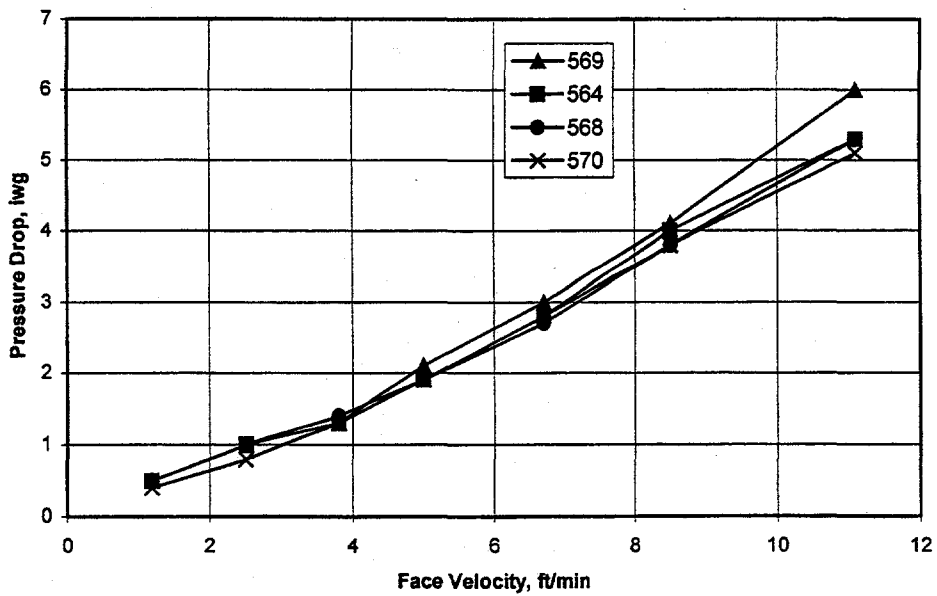


Figure 35 - PRD-66M - Room temperature gas flow resistance<sup>12</sup>

During April 1997, one candle of each membrane type was subjected to a high temperature, high pressure (HTHP), simulated pressurized fluidized-bed combustion (PFBC) environment. Testing included exposure of the PRD-66 candles with alternate monolithic and advanced fiber reinforced candle filter elements in order to support pressurized circulating fluidized-bed combustion (PCFBC) test initiatives in Karhula, Finland. The filter array was subjected to 120 hours of steady state operating conditions at 843°C (1550°F), and subsequently 2,200 accelerated pulse cycles, and 12 mild thermal transient events.

Post-test inspection of the filter array indicated that both exposed PRD-66 filter elements remained intact. The following comments were noted:

- thin dust cake layer on both considered to be a "normal conditioned layer"
- no debonding or "divoting" of the outer membrane occurred
- no cracks were identified along the flange or body
- apparent heavier retention of fines in diamond pattern of PRD-66C versus PRD-66M

Post-test gas flow resistance measurements of the qualification-tested candles are provided in Figure 36. The coarse membrane (PRD-66C) element initially had a lower pressure drop in comparison to the medium membrane (PRD-66M) element; after qualification testing, this relationship was retained. These elements were subsequently subjected to mechanical strength characterization, x-ray diffraction, and microstructural analysis.

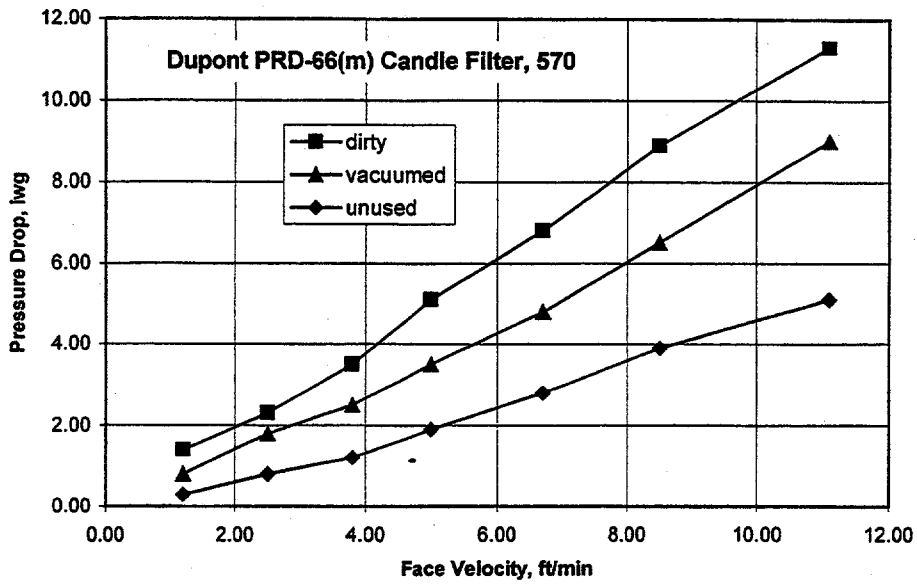


Figure 36 - Gas flow resistance of as-manufactured and HTHP-exposed PRD-66M elements<sup>12</sup>

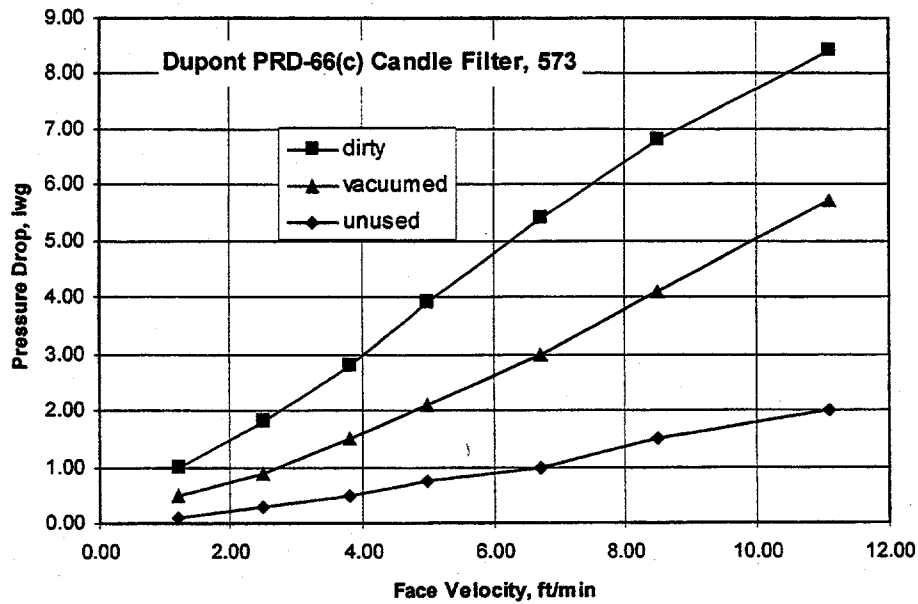


Figure 37 - Gas flow resistance of as-manufactured and HTHP-exposed PRD-66C elements<sup>12</sup>

W-STC characterized the mechanical properties the two tested elements, along with one as-manufactured candle of each membrane type (see Appendix 2). Table 11 summarizes the compressive and tensile c-ring tests that were conducted; the data suggests that the strength of the coarse and medium membrane "exposed" elements tended to be greater than the strength of comparable as-manufactured elements. M. A. Alvin of W-STC feels that this conclusion is supported by similar results obtained during other simulated and field exposures.<sup>4</sup> It had been postulated that an increase in strength could result from the bulk versus barrier filtration characteristics of the material, whereby submicron and micron fines penetrate through the membrane of the PRD-66 filter element and become trapped within the filter wall. Under these conditions, trapped ash could cause significant problems during field operation, particularly if thermal expansion occurs within the filter wall during plant startup cycles,<sup>5</sup> or hydration of the ash resulted during thermal shutdown cycles (Section 3.3.3). In relation to alternate filter elements,<sup>6</sup> the PRD-66 candle filters were considered to be "moderately low" load-bearing (Table 12). Additional material properties as burst strength, modulus, and Poisson's ratio, which were developed at Westinghouse, are provided in Table 13.

ROOM TEMPERATURE AND PROCESS STRENGTH OF THE AS-MANUFACTURED AND QUALIFICATION-TESTED DUPONT PRD-66 CANDLE FILTERS					
Candle Identification Number	Status	C-Ring Compressive Strength, psi		C-Ring Tensile Strength, psi	
		25-degC	843-degC	25-degC	843-degC
DuPont PRD-66 (Coarse Membrane)					
D-563c	As-Manufactured	955+/-62 (9)	962+/-92 (8)	809+/-154 (9)	1009+/-103 (7)
D-573c	Qualification Tested	1214+/-67 (9)	1210+/-86 (9)	990+/-82 (9)	1195+/-166 (9)
DuPont PRD-66 (Medium Membrane)					
D-564m	As-Manufactured	990+/-130 (9)	883+/-79 (9)	846+/-105 (9)	918+/-104 (9)
D-570m	Qualification Tested	1021+/-127 (9)	1019+/-88 (9)	973+/-165 (9)	1193+/-149 (8)

Table 11 - W-STC Room temperature and process strength of PRD-66 elements <sup>12</sup>

ULTIMATE LOAD APPLIED DURING STRENGTH CHARACTERIZATION OF THE AS-MANUFACTURED AND QUALIFICATION-TESTED DUPONT PRD-66 CANDLE FILTERS					
Candle Identification Number	Status	C-Ring Compressive Load-to-Failure, psi		C-Ring Tensile Load-to-Failure, psi	
		25-degC	843-degC	25-degC	843-degC
DuPont PRD-66 (Coarse Membrane)					
D-563c	As-Manufactured	8.2+/-0.5 (9)	8.2+/-0.9 (8)	5.2+/-1.1 (9)	6.7+/-0.7 (7)
D-573c	Qualification Tested	10.3+/-0.6 (9)	10.3+/-0.6 (9)	6.4+/-1.2 (9)	7.6+/-1.0 (9)
DuPont PRD-66 (Medium Membrane)					
D-564m	As-Manufactured	8.0+/-0.9 (9)	7.3+/-0.6 (9)	5.2+/-0.6 (9)	5.7+/-0.6 (9)
D-570m	Qualification Tested	8.3+/-1.0 (9)	8.3+/-0.8 (9)	6.1+/-0.9 (9)	7.4+/-0.8 (8)

Table 12 - W-STC Ultimate load applied during strength characterization <sup>12</sup>

MATERIAL PROPERTIES OF THE AS-MANUFACTURED AND QUALIFICATION-TESTED DUPONT PRD-66 CANDLE FILTERS					
Candle Identification Number	Status	Burst Pressure, psi	Ultimate Hoop Stress, psi	Modulus, psi x 10 <sup>6</sup>	Poisson's Ratio
DuPont PRD-66 (Coarse Membrane)					
D-563c	As-Manufactured	148	555	7.96	0.86
D-573c	Qualification Tested	158	597	6.11	0.82
DuPont PRD-66 (Medium Membrane)					
D-564m	As-Manufactured	180	691	7.09	0.84
D-570m	Qualification Tested	170	653	5.42	0.84

Table 13 - W-STC Material properties of PRD-66 elements <sup>12</sup>

Additional strength testing was conducted by DuPont Lanxide Composites on segments of the same "exposed" filter elements tested by W-STC and on two different as-manufactured candles. These results, shown in Table 14, DO NOT support the Westinghouse conclusions. The "exposed" PRD-66C had a higher strength, however the "exposed" PRD-66M had a lower strength. The data suggests that the candle-to-candle strength variability of the material outweighs any effect of exposure. It was interesting to note, however, that the W-STC c-ring strength values and the DLC o-ring strength values for candles #570 and #573 were very similar.

Candle ID#	Status	O-Ring Comp.Str	Load-to-Failure
PRD-66C			
566C	As-Manufactured	1087 ± 80 (11)	41.5 ± 3.1 (11)
573C	Qualification Tested	1252 ± 44 (5)	45.6 ± 3.6 (5)
PRD-66M			
567M	As-Manufactured	1229 ± 117 (11)	44.7 ± 3.9 (11)
570M	Qualification Tested	1095 ± 184 (5)	37.2 ± 6.7 (5)

Table 14 - DLC Diametrical compression testing of HTHP-exposed & unexposed candles

### 3.6.2 PCFBC Exposure at Karhula

A 581-hour exposure of PRD-66C filter elements was conducted in Foster Wheeler's pressurized circulating fluidized-bed combustion (PCFBC) test facility in Karhula, Finland. Analysis of an exposed filter was conducted under Task 3.2.

Seven candles began the test in early September. Table 15 (provided by Westinghouse) identifies the operating conditions experienced by the PRD-66C Hot Gas Candle Filters in Westinghouse's Advanced Particulate Filter cluster during the TS2-1997 test campaign

<b>Pressurized Circulating Fluidized-bed Combustion Testing at the Foster Wheeler Test Facility in Karhula, Finland - TS2-97</b>	
Date	September 4, 1997 – November 7, 1997
Number of Filter Elements Tested	8
Filter Operating Temperature, deg.C	700 - 750
Filter Operating Pressure, bar	9.5 - 11
Coal Feed	Eastern Kentucky
Sorbent	Florida Limestone
Time, hrs	581 (6)*, 342 (1), 239 (1)
Face Velocity, cm/sec	2.8 - 4.0
Particle Load, ppmw	6000 - 9000
Particle Size, microns	< 1 - 150
Thermal Excursions	None
Number of Startup/Shutdown Cycles	7

\* The number in parentheses indicates the number of elements exposed for the respective operating hours.

Table 15 - Karhula PCFBC test conditions

After 239 hours, the system was turned off and all elements were examined. Significant quantities of ash were found on the "clean side" of the system. All candles were removed and cleaned by vacuuming and washing. One PRD-66C candle broke at the flange when it was removed;

some force had been necessary to dislodge the flange from the holder assembly. When the run was restarted, a new PRD-66C candle was put in its place. The test concluded 342 hours later.

At the conclusion of the run, the six PRD-66C elements that were exposed for the entire 581 hours, and the one candle that was exposed for a total of 342 hours, all looked good. All but one of the elements had been cleaned by brushing and vacuuming prior to inspection, see photograph in Figure 38. There was no sign of any material deterioration in the possible forms of "divots", abrasion, poor membrane adhesion, or cracking. A significant amount of ash, however, was observed in the wall of the inside diameter, though it was much less for the element that was only exposed for 342 hours.

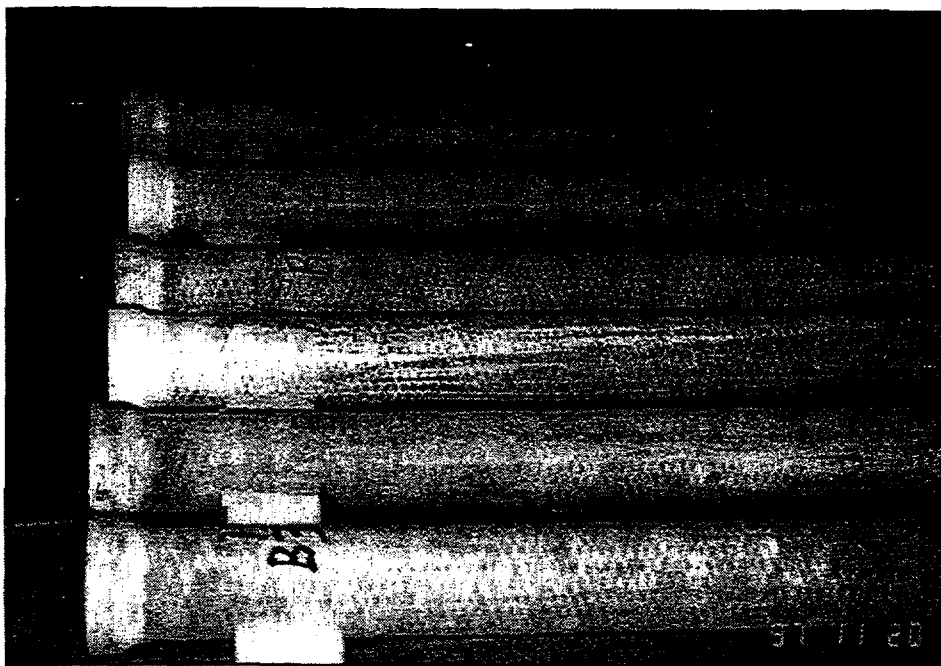
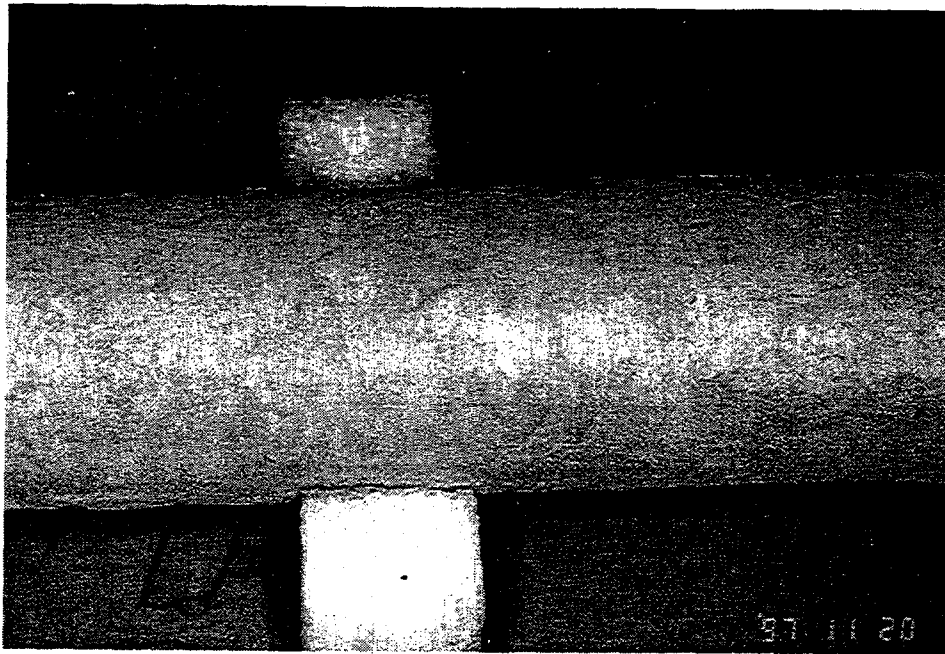


Figure 38 - Karhula-exposed PRD-66C filters

A single candle was examined before any ash had been cleaned from the material. A conditioned ash cake layer, approximately 2mm thick, had formed along the outside diameter, see photograph in Figure 39. The ash was soft and easily removable by handling or by brushing. The inside diameter was also caked with ash, approximately 2mm thick, with at least six inches of loose ash present in the tip of the candle.



**Figure 39 - Outside diameter of Karhula-exposed element before ash removal**



**Figure 40 - Inside diameter of Karhula-exposed element before ash removal**

All candles were vacuum-cleaned, inside and out, prior to inspection, after which, differential pressure measurements were conducted by Foster Wheeler personnel, see Figure 41. In summary, all elements showed significantly higher backpressure, with the exception of the single candle that was installed after the "239-hour shutdown", which had a slight increase in backpressure.

FW has attributed the plugging of the other filters to the presence of significant quantities of ash on the “clean side”, rather than the length of exposure.

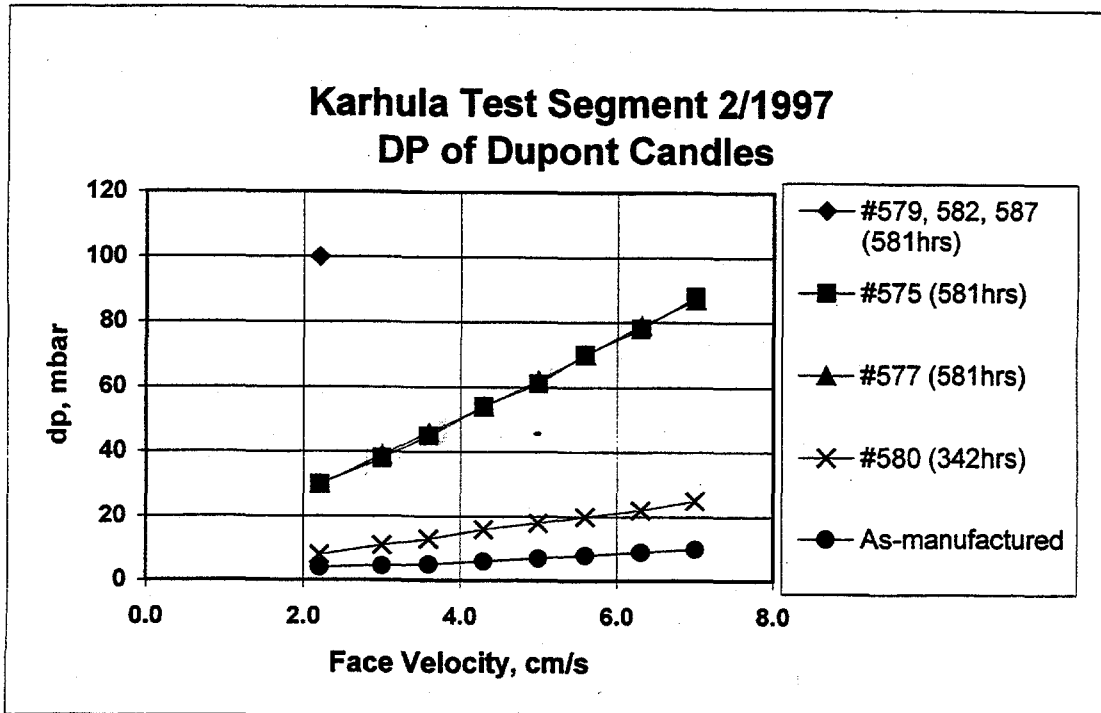


Figure 41 - Differential pressure of Karhula filters measured by Foster Wheeler

One of the candles with the full exposure time (#577), and the candle, which broke during removal after 239 hours (#591), were shipped to DLC for analysis. Unfortunately, both broke into at least three pieces during transport.

### 3.6.2.1 Visual Inspection for Ash Penetration in Karhula-Exposed Element

Samples of candle #577 (with 581 exposure hours) were prepared by “fast-fracture”, to expose a cross-section of the wall. The contrast between the dark (orange-brown) ash and the white PRD-66 support material made it easy to determine where obvious ash penetration had occurred. Figure 42 is a photograph of a particular sample in which the support yarn was exposed at two distinct levels: just below the membrane and approximately 4mm below the membrane (mid-way through the wall). The presence of ash mid-way through the wall was no surprise, since a process upset had occurred during the Karhula exposure, which introduced large quantities of ash into the ID of the filter elements. The most significant observation was that there was no ash within 1-2mm of the membrane. Figure 43 is an enlargement of that area shown in Figure 42. The ash is clearly seen trapped in the membrane, while the yarns of the support structure immediately below are clean and white. This indicates that the new PRD-66C membrane (with nominal 25-micron pores) is an

effective surface filter for PCFBC applications. It is significant that, no "divots" occurred despite the large volumes of ash that penetrated from the "clean side".

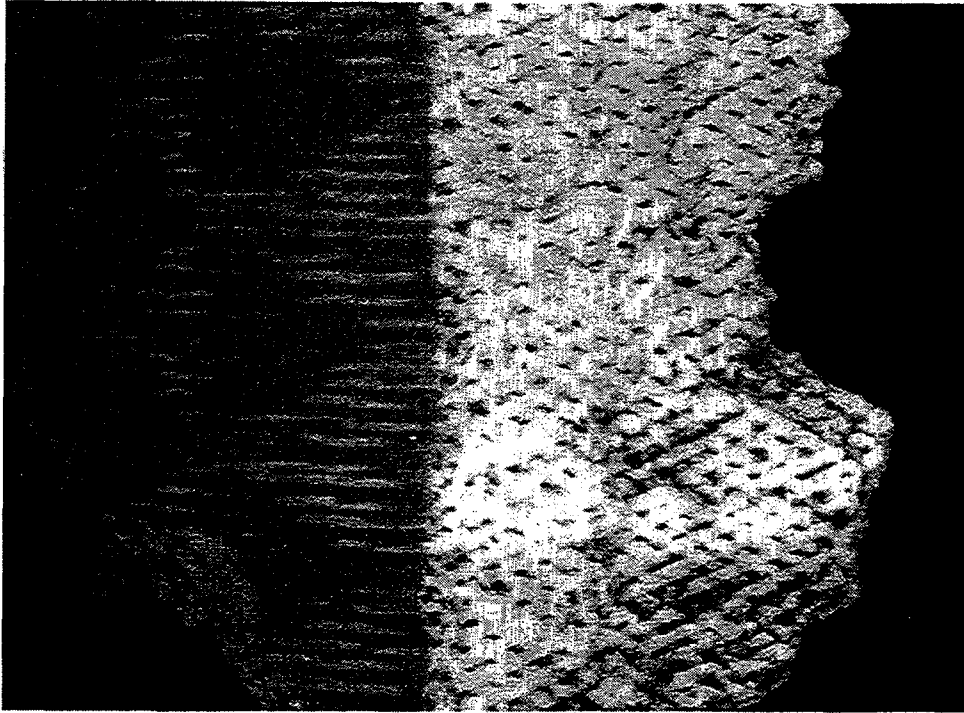


**Figure 42 - Wall interior of Karhula-exposed candle #577**

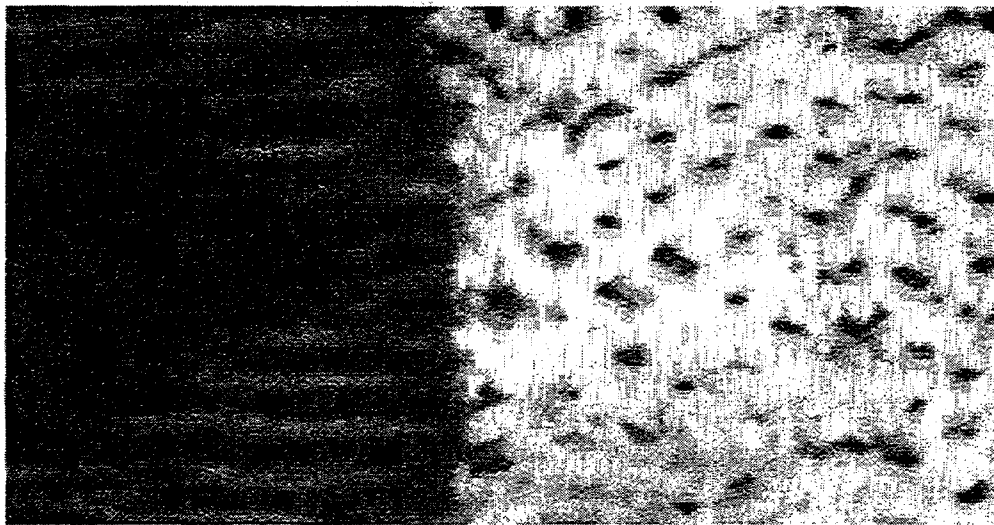


**Figure 43 - Close-up of #577 - OD surface and 1-2mm below**

FW also shipped approximately one liter of PCFBC ash that could be used to conduct a particle infiltration test (PIT) on a "sister" candle filter. The test was performed on a two-inch segment of unused candle #576. The results confirmed the observations made on the Karhula-exposed candle; no penetration of ash through the membrane was detected.

### 3.6.2.2 *Microstructural Analysis of Karhula-Exposed and Unexposed Elements*

A series of scanning electron microscopy (SEM) photographs were taken of different features of the exposed candle #577 and the unexposed candle #576.

In the following photos, comparisons were made of the exposed outside diameter surfaces. In Figure 44, the structure of the unexposed membrane has coarse alumina grains speckled with fine grains of the fusible binder, when viewed at 300X. By comparison, the exposed candle in Figure 45 and Figure 46 show similar irregularities which have been "smoothed-over" by the presence of ash.



**Figure 44 - 300X - UNEXPOSED candle surface**

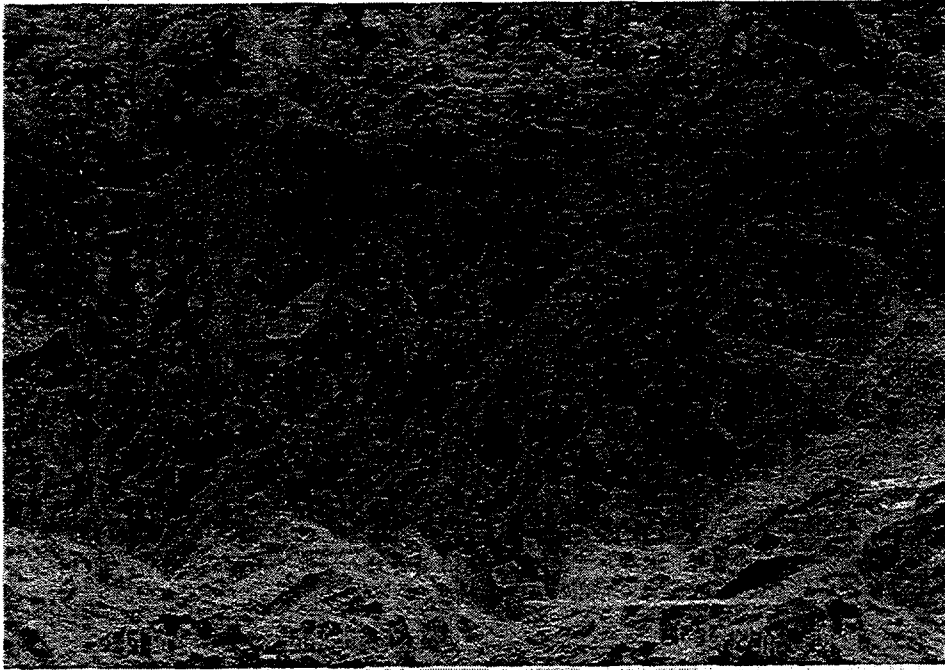


**Figure 45 - 300X - EXPOSED candle surface**



**Figure 46 - 1,000X - EXPOSED candle surface**

In the following photos, cross-sections of the particulate membrane filler were exposed by fast-fracture and evidence of any ash deposits were sought. By making comparisons with an unexposed filter (Figure 47), no obvious trace of ash could be discerned in Figure 48; no significant difference in the sharp edges of the alumina particles of the membrane was observed. Mary Anne Alvin, of Westinghouse, has suggested that an elemental scan for calcium would be more conclusive.

but the high amount of gold coating necessary on the sample for SEM obscures the calcium peaks. The assistance of an outside lab would be required and, unfortunately, was not budgeted for.



**Figure 47 - UNEXPOSED CANDLE, cross-section of membrane filler (300X)**

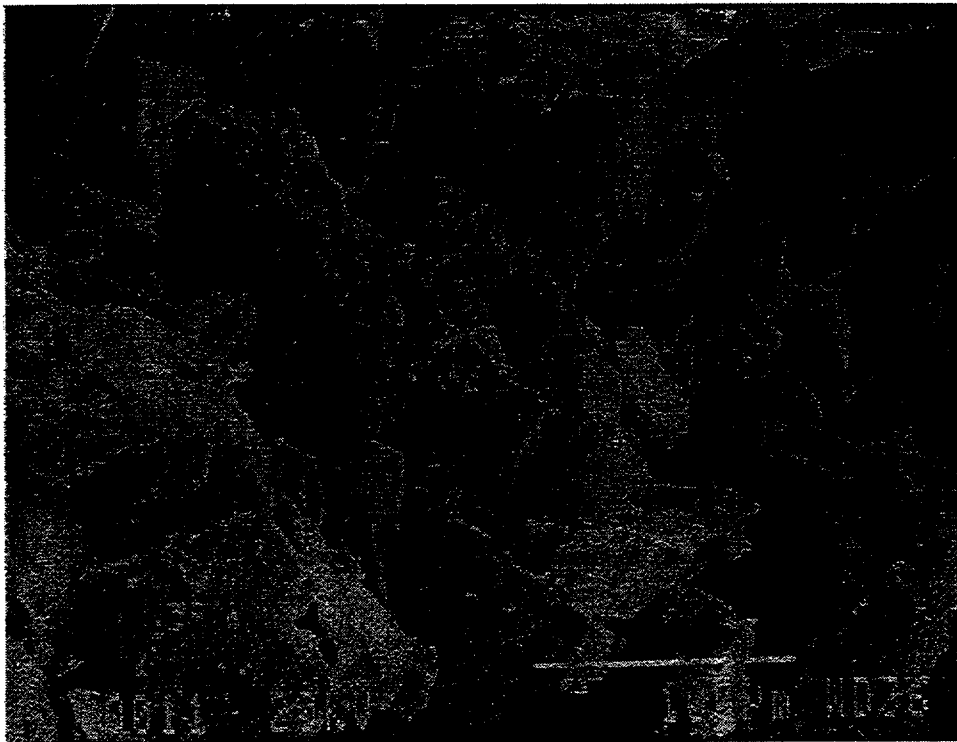


**Figure 48 - EXPOSED CANDLE, cross-section of membrane filler (300X)**

In the following photos, the SEM was focused on the region of the support wall within 3mm of the OD surface. The exposed candle in Figure 50 showed no obvious evidence of ash entrainment when compared to the unexposed candle in Figure 49.

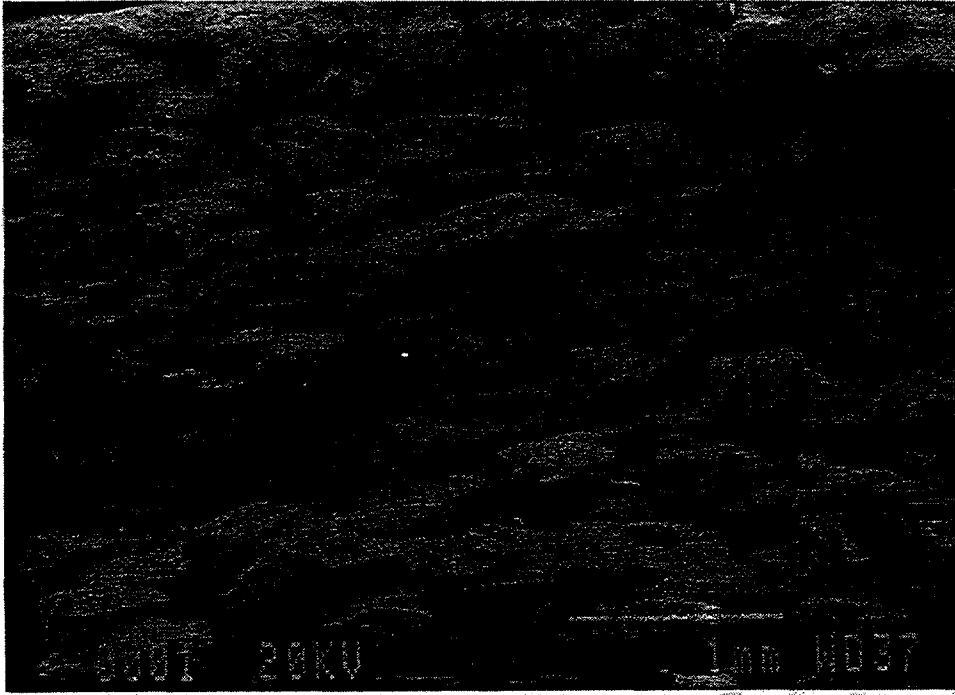


**Figure 49 - 25X, fast-fracture - UNEXPOSED CANDLE, interior of support wall**

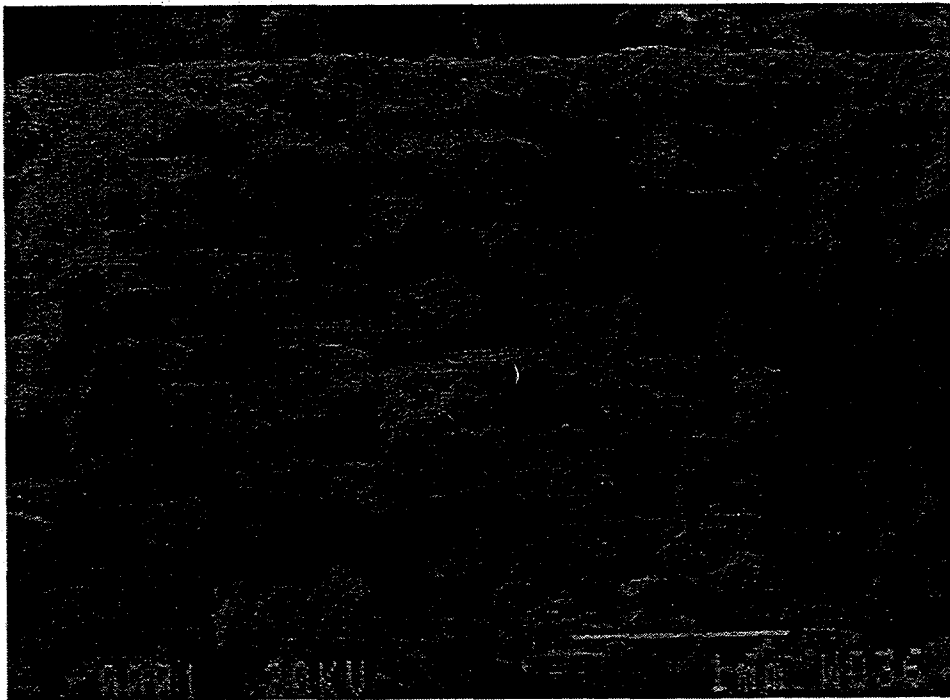


**Figure 50 - 25X, fresh-fracture - EXPOSED CANDLE, interior of support wall**

Upon closer examination of the 1mm area directly below the membrane, the natural microcracks in the unexposed material are visible along the surface of the filament structures (Figure 51). These microcracks were also visible in the Figure 52 photo of the exposed candle; if ash penetration had occurred, a smoothening or filling of those features may have resulted. These micrographs support the observation that no detectable penetration of ash through the membrane layer occurred.



**Figure 51 - 50X, fast-fracture - UNEXPOSED CANDLE, interior of support wall**

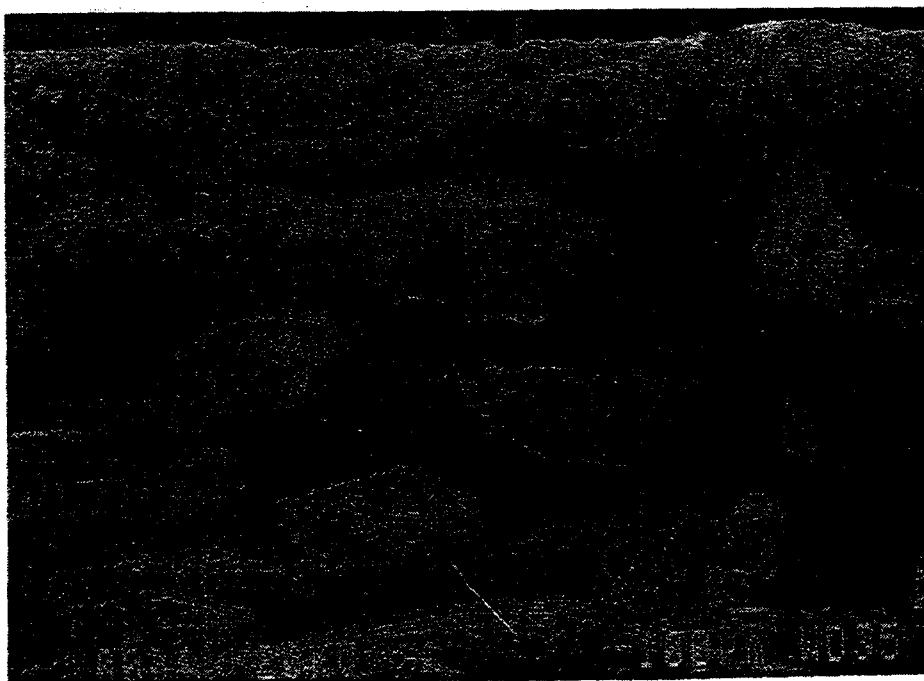


**Figure 52 - 50X, fast-fracture - EXPOSED CANDLE, interior of wall support**

In Figure 53 through Figure 56, the conditions of the filament structures were examined for evidence of any change resulting from the exposure environment. Figure 53 and Figure 54 each show the cross-section of a single "yarn bundle" at 300X magnification. Each yarn bundle originally consisted of hundreds of filaments. During the firing process, the individual amorphous filaments, coated with alumina, are converted to crystalline phases, primarily cordierite and alumina, with some mullite. The mullite is evident as "needle-shaped" crystals, as seen in the higher magnification photos (Figure 55 and Figure 56). Under conditions which challenge the stability of the PRD-66 microstructure, these needle-like formations are the first to degrade and holes begin to form in the centers of the individual yarn filaments. Neither sign of reaction was observed in either photo of the exposed candle. As a result of this analysis, it was concluded that the microstructure of the PRD-66 material was stable in the Karhula PCFBC environment.



**Figure 53 - UNEXPOSED CANDLE, individual "yarn bundle" (300X)**

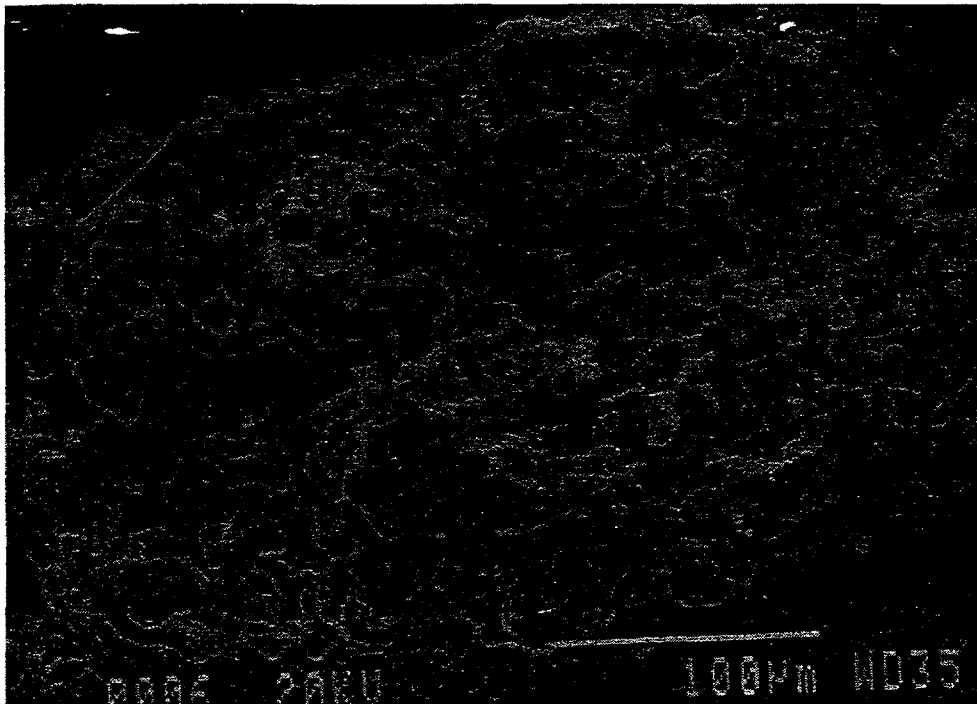


**Figure 54 - EXPOSED CANDLE, individual "yarn bundle" (300X)**

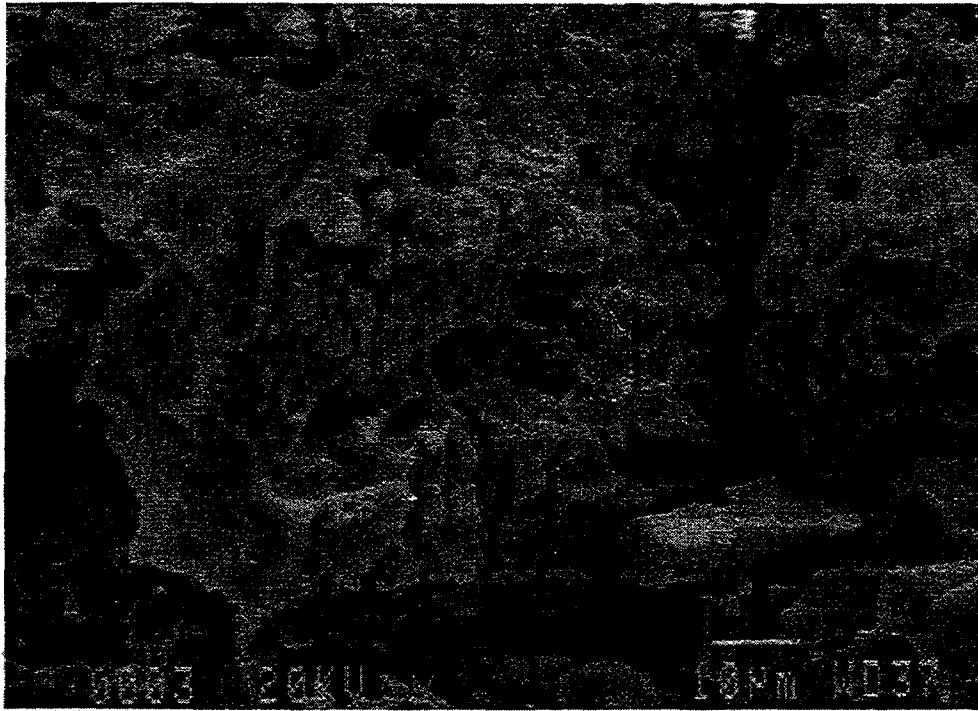


**Figure 55 - UNEXPOSED CANDLE, individual "yarn bundle" (1,000X)**



**Figure 56 - EXPOSED CANDLE, individual "yarn bundle" (1,000X)**

### 3.6.2.3 Diffraction Analysis of Karhula-Exposed and Unexposed Elements

The stability of the PRD-66 material was further evaluated by qualitative x-ray diffraction (XRD). Specimens of candle #576 (unexposed) and candle #576 (581-hr exposure) were ground into powder and scanned from 5-90 degrees two theta. Both samples contained alumina, cordierite, mullite, and small amounts of cristobalite, in virtually identical amounts. The "exposed" material showed no evidence of any other crystalline phases that may have formed from a reaction of the PRD-66 with the PCFBC environment. The presence of coal ash in the "exposed" sample was not apparent since the material is not crystalline in nature. This analysis supports the visual SEM observation that the material was stable under the Karhula PFBC conditions.

### 3.6.2.4 Strength Testing of Karhula-Exposed and Unexposed Elements

As previously mentioned, two tested filter elements had been returned by Foster Wheeler to DLC. Candle #577 had been exposed to 581 hours on coal. Candle #591 had been exposed to 239 hours on coal and was broken at the flange when all candles were removed from the vessel for cleaning. 1-inch wide o-rings were sectioned from each candle and tested by o-ring diametrical compression. Average strengths and "load-to-failure" values are compared to unused candles as shown in Table 16. No apparent change in strength was observed.

Unit No.	Condition	Average (psi)	Std. Dev. (psi)	Load-to-Failure (lbs.)	Samples
C566	Unexposed	1087.6	80.8	41.5	11
C576	Unexposed	1256.2	64.7	45.6	6
C578	Unexposed	1352.9	65.2	48.1	5
C590	Unexposed	1076.1	47.8	47.4	6
C577	Exposed-581hrs	1246.6	49.9	50.0	6
C591	Exposed-239hrs	1315.0	103.9	57.0	6

Table 16 - O-ring diametrical compressive testing of Karhula-exposed & unexposed candles